Table VII. Deviation of Selected Atoms from Selected Planes

Plane	Atom	Deviation of atom from plane, Å	Atom	Deviation of atom from plane, Å
MnB(1)B(2)	H(1)	0.172	H(5)	−0.568
	H(2)	−0.293	H(7)	−0.847
	H(4)	−0.364		
MnB(1)B(3)	H(1)	0.529	H(6)	0.490[a,b]
	H(3)	0.471	H(7)	−1.140
	H(5)	0.425[a,b]	H(8)	−1.126
MnB(2)B(3)	H(2)	0.245	H(6)	0.369
	H(3)	−0.078	H(8)	0.756
	H(4)	0.561		
B(1)B(2)B(3)	H(1)	−0.621	H(5)	1.123
	H(2)	−0.660	H(6)	1.106
	H(3)	−0.732	H(7)	−0.275[c,d]
	H(4)	1.146	H(8)	−0.282[c,d]

[a] In $(Ph_3P)_2CuB_3H_8$ these bridge hydrogens are 0.38 and 0.40 Å above the CuB(1)B(3) plane.[9d] [b] In $Be(B_3H_8)_2$ these bridge hydrogens are displaced an average of 0.092 Å above the BeB(1)B(3) plane.[13] [c] In $(Ph_3P)_2CuB_3H_8$ these bridge hydrogens are +0.2 and −0.8 Å out of the plane defined by the boron atoms. [d] In $Be(B_3H_8)_2$ these bridge hydrogens are an average of 0.026 Å out of the B(1)B(2)B(3) plane.

of the unit cell in Figure 3. The $(CO)_3MnB_3H_8$ exists as discrete molecules and exhibits normal van der Waals packing with the cocrystallized toluene molecules. The closest distance of 3.202 Å is between carbonyl oxygen atoms of adjacent molecules, while the closest toluene nonbonding distance is 3.753 Å from the toluene methyl carbon C(1) and B(2) of an adjacent molecule.

Acknowledgment. This work has been supported in part by grants from the National Science Foundation.

Registry No. $(CO)_3MnB_3H_8$, 53801-96-0; $(CO)_4MnB_3H_8$, 53801-97-1.

Supplementary Material Available: A listing of observed and calculated structure factor amplitudes (9 pages). Ordering information is given on any current masthead page.

References and Notes

(1) D. F. Gaines and S. J. Hildebrandt, *J. Am. Chem. Soc.*, **96**, 5574 (1974). The solution structure of $(CO)_3MnB_3H_8$ is discussed in greater detail in ref 3.

(2) D. F. Shriver, "The Manipulation of Air-Sensitive Compounds", McGraw-Hill, New York, N.Y., 1969.

(3) D. F. Gaines and S. J. Hildebrandt, *Inorg. Chem.*, companion paper in this issue.

(4) "International Tables for X-Ray Crystallography", Vol. I, 2nd ed, The Kynoch Press, Birmingham, England, 1965, p 99.

(5) Programs used in the structural determination and refinement included ORFLS and ORFFE, the W. P. Busing, K. O. Martin, and H. A. Levy least-squares and error analysis programs; and ORTEP 2, the C. K. Johnson thermal ellipsoid plotting program. All other crystallographic programs used were written by J.C.C.

(6) $R_1 = \sum(|F_o| - |F_c|)/\sum|F_o|$; $R_2 = [\sum w_i(|F_o| - |F_c|)^2/\sum w_i|F_o|^2]^{1/2}$. The standard deviation of an observation of unit weight is defined as $[w_i(|F_o| - |F_c|)^2/(m - n)]^{1/2}$, where m is the number of observations and n is the number of parameters fitted to the data.

(7) H. P. Hanson, F. Herman, J. D. Lea, and S. Skillman, *Acta Crystallogr.*, **17**, 1040 (1964).

(8) R. F. Stewart, E. R. Davidson, and W. T. Simpson, *J. Chem. Phys.*, **42**, 3175 (1965).

(9) (a) L. J. Guggenberger, *Inorg. Chem.*, **9**, 367 (1970); (b) F. Klanberg, E. L. Muetterties, and L. J. Guggenberger, *ibid.*, **7**, 2272 (1968); (c) S. J. Lippard and D. A. Ucko, *ibid.*, **7**, 1051 (1968); (d) S. J. Lippard and K. M. Melmed, *ibid.*, **8**, 2755 (1969); (e) E. L. Muetterties, W. G. Peet, P. A. Wegner, and C. W. Alegranti, *ibid.*, **9**, 2447 (1970); (f) F. Klanberg and L. J. Guggenberger, *Chem. Commun.*, 1293 (1967); (g) D. F. Gaines and J. H. Morris, *ibid.*, 626 (1975); (h) H. Beall, C. H. Bushweller, W. J. Dewkett, and M. Grace, *J. Am. Chem. Soc.*, **92**, 3484 (1970); (i) C. H. Bushweller, H. Beall, M. Grace, W. Dewkett, and H. Bilofsky, *ibid.*, **93**, 2145 (1971); (j) J. Borlin and D. F. Gaines, *ibid.*, **94**, 1367 (1972); (k) S. Hermanek and J. Plesek, *Collect. Czech. Chem. Commun.*, **31**, 177 (1966).

(10) An additional mode of bonding, π-borallyl, is encountered when the ligand is $B_3H_7^{2-}$: (a) A. R. Kane and E. L. Muetterties, *J. Am. Chem. Soc.*, **93**, 1041 (1971); (b) L. J. Guggenberger, A. R. Kane, and E. L. Muetterties, *ibid.*, **94**, 5665 (1972).

(11) (a) H. D. Kaesz, W. Fellmann, G. R. Wilkes, and L. F. Dahl, *J. Am. Chem. Soc.*, **87**, 2753 (1965); (b) J. W. Lott, D. F. Gaines, H. Shenhav, and R. Schaeffer, *ibid.*, **95**, 3042 (1973); (c) J. C. Calabrese, M. B. Fischer, D. F. Gaines, and J. W. Lott, *ibid.*, **96**, 6318 (1974); (d) J. W. Lott and D. F. Gaines, *Inorg. Chem.*, **13**, 2261 (1974); (e) D. F. Gaines, J. W. Lott, and J. C. Calabrese, *ibid.*, **13**, 2419 (1974).

(12) (a) L. F. Dahl and R. E. Rundle, *Acta Crystallogr.*, **16**, 419 (1963); (b) S. J. LaPlaca, W. C. Hamilton, J. A. Ibers, and A. Davison, *Inorg. Chem.*, **8**, 1928 (1969).

(13) J. C. Calabrese, D. F. Gaines, S. J. Hildebrandt, and J. H. Morris, *J. Am. Chem. Soc.*, **98**, 5489 (1976).

(14) C. R. Peters and C. E. Nordman, *J. Am. Chem. Soc.*, **82**, 5738 (1960).

(15) W. N. Lipscomb, "Boron Hydrides", W. A. Benjamin, New York, N.Y., 1963, p 110.

(16) F. A. Cotton and G. Wilkinson, "Advanced Inorganic Chemistry", 3rd ed, Wiley, New York, N.Y., 1972, p 683.

(17) W. N. Lipscomb, "Boron Hydrides", W. A. Benjamin, New York, N.Y., 1963, Chapter 2.

(18) K. Wade, *Adv. Inorg. Chem. Radiochem.*, **18**, 1 (1976).

(19) C. Glidewell, *Inorg. Nucl. Chem. Lett.*, **11**, 761 (1975).

Contribution from the Department of Chemistry,
University of Wisconsin, Madison, Wisconsin 53706

Syntheses and Properties of Some Neutral Octahydrotriborate(1−) Complexes of Chromium-, Manganese-, and Iron-Group Metals

DONALD F. GAINES* and STEVEN J. HILDEBRANDT

Received August 30, 1977

Reaction of selected complexes of the type $L_n(CO)MX$ with salts and derivatives of $B_3H_8^-$ has produced $(CO)_4MnB_3H_8$, $(CO)_4ReB_3H_8$, $(\eta^5\text{-}C_5H_5)(CO)FeB_3H_8$, $(H)(CO)_3FeB_3H_8$, $(\eta^5\text{-}C_5H_5)(CO)_2MoB_3H_8$, $(\eta_5\text{-}C_5H_5)(CO)_2WB_3H_8$, $[(C_6H_5)_3]P(CO)_3MnB_3H_8$, and $[(C_6H_5)_2PCH_2CH_2P(C_6H_5)_2](CO)_2MnB_3H_8$. In these complexes $B_3H_8^-$ is a bidentate ligand via two M–H–B bridge hydrogen bonds. $(CO)_4MnB_3H_8$ undergoes reversible decarbonylation yielding $(CO)_3MnB_3H_8$, in which the $B_3H_8^-$ ligand is tridentate. $(CO)_4MnB_3H_8$ reacts with Br_2 and Cl_2 to produce $(CO)_4MnB_3H_7Br$ (or Cl), the halogen substitution occurring at the boron atom not bound to manganese. Detailed ^{11}B and ^1H NMR studies of these complexes reveal their structures and some examples of interesting selective intramolecular hydrogen exchange phenomena.

Introduction

Several main-group and transition-metal complexes containing the octahydrotriborate(1−) ligand, $B_3H_8^-$, have been reported during the last decade. Representative examples include $[(C_6H_5)_3P]_2CuB_3H_8$,[1] $(C_5H_5)_2TiB_3H_8$,[2a] $[(CO)_4CrB_3H_8^-]$,[2] $(CH_3)_2GaB_3H_8$,[3] and $Be(B_3H_8)_2$.[4] Single-crystal x-ray studies of three[1c,2c,4b] of these complexes show that the bidentate $B_3H_8^-$ ligand is bound to metals via two M–H–B three-center two-electron bridge hydrogen bonds from adjacent boron atoms. Spectroscopic studies suggest similar static structures for all $M–B_3H_8$ complexes except $(CO)_3MnB_3H_8$, vide infra. Some of the complexes have low barriers to partial

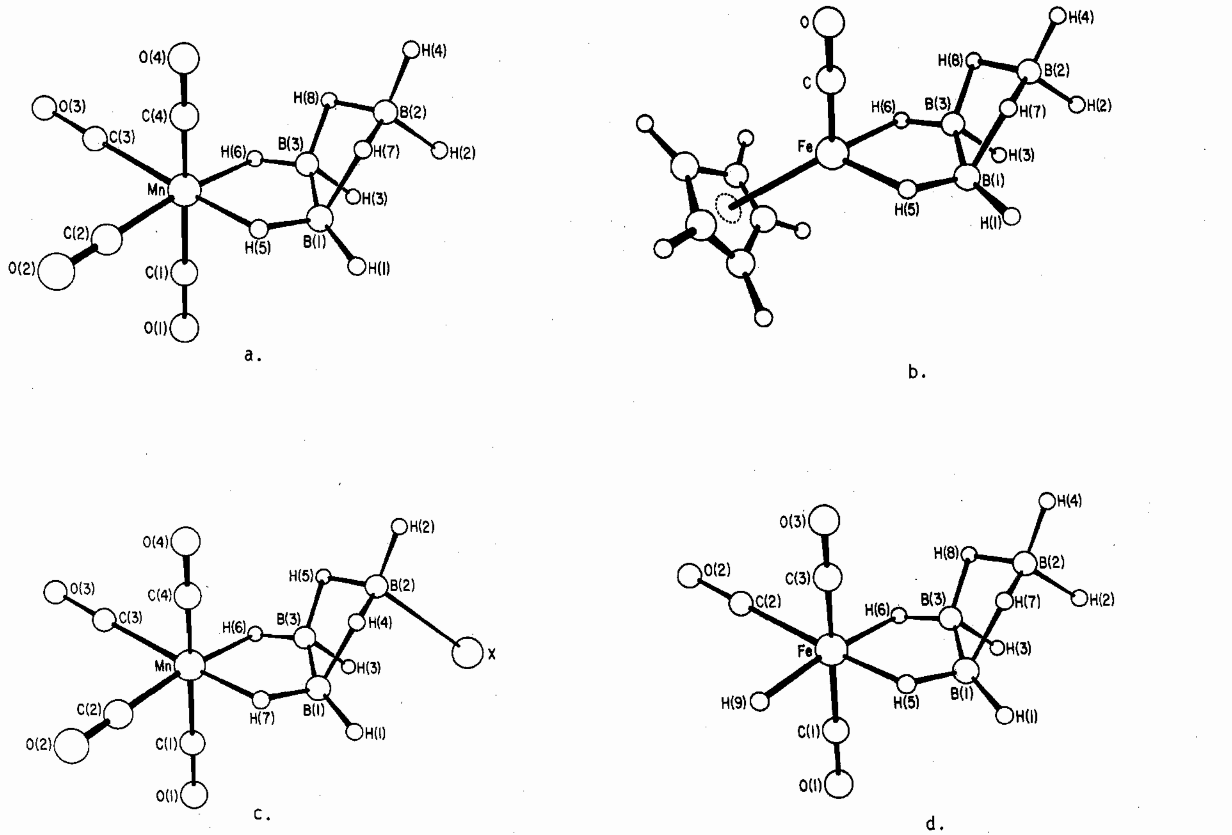

Figure 1. Proposed structures for (a) $(CO)_4MnB_3H_8$, (b) $(\eta^5\text{-}C_5H_5)(CO)FeB_3H_8$, (c) $(CO)_4MnB_3H_7X$ (one of the possible isomers), and (d) $(H)(CO)_3FeB_3H_8$.

or complete intramolecular exchange within the $B_3H_8^-$ ligand and have been the subject of detailed NMR studies.[1-4]

We present here the syntheses of several neutral $B_3H_8^-$ complexes of chromium-, manganese-, and iron-group metals and illustrate some of their chemical and spectroscopic properties. Chemical studies have been largely restricted to $(CO)_4MnB_3H_8$, the most versatile complex in this study. The accompanying NMR studies illustrate that the presence or absence of intramolecular hydrogen exchange in the $B_3H_8^-$ ligands and the mechanisms of such exchanges are influenced by a number of subtle, ill-defined factors.

Results and Discussion

Preparation of Metal–B_3H_8 Complexes. The most general method of preparation of metal–B_3H_8 complexes involves the reaction of an organometallic halide with $(CH_3)_4NB_3H_8$ in methylene chloride solution (Table I).

$$L_n(CO)MX + (CH_3)_4NB_3H_8 \rightarrow L_nMB_3H_8 + CO + (CH_3)_4NX$$

$M = Mn, Re, Mo, W, Fe$

$L = CO, \eta^5\text{-}C_5H_5, (C_6H_5)_3P, (C_6H_5)_2PCH_2CH_2P(C_6H_5)_2$

$X = Cl, Br, I$

In practice other ionic $B_3H_8^-$ salts, as well as covalent main-group compounds, can be used successfully in place of $(CH_3)_4NB_3H_8$. Most reactions proceed smoothly at room temperature, though thermal or photolytic induction is required in some cases. All of the preparations are accompanied by the evolution of 1 equiv of carbon monoxide per equivalent of organometallic reagent. Since most syntheses are performed in vacuo it is possible to monitor the extent of reaction simply by observing the carbon monoxide evolution. The following new metal derivatives of the $B_3H_8^-$ ion have been prepared: $(CO)_4MnB_3H_8$, $(CO)_4ReB_3H_8$, $(\eta^5\text{-}C_5H_5)(CO)FeB_3H_8$, $(H)(CO)_3FeB_3H_8$, $(\eta_5\text{-}C_5H_5)(CO)_2MoB_3H_8$, $(\eta_5\text{-}C_5H_5)(CO)_2WB_3H_8$, $[(C_6H_5)_3P](CO)_3MnB_3H_8$, and $[(C_6H_5)_2PCH_2CH_2P(C_6H_5)_2](CO)_2MnB_3H_8$.

Table I. Selected Preparation Procedures for $(CO)_4MnB_3H_8$

Triborohydride reagent	Manganese substrate	Solvent	Temp,[a] °C	Reacn time, h	Yield, %
$(CH_3)_4NB_3H_8$	$Mn(CO)_5Br$	CH_2Cl_2	RT	80	65–80
CsB_3H_8	$Mn(CO)_5Br$	$(C_2H_5)_2O$	RT	70	53
TlB_3H_8	$Mn(CO)_5Br$	CH_2Cl_2	RT	19	77
$(CH_3)_2AlB_3H_8$	$Mn(CO)_5Br$, $Mn(CO)_5I$	None	RT → 70	1	<5
$(CH_3)_2AlB_3H_8$	$Mn(CO)_5Br$	CH_2Cl_2	RT	22	37
$(CH_3)_2GaB_3H_8$	$Mn(CO)_5Br$, $Mn(CO)_5I$	None	RT → 70	1	30
$(CH_3)_2GaB_3H_8$	$Mn(CO)_5Br$	$(C_2H_5)_2O$	RT	20	26
$(CH_3)_2GaB_3H_8$	$Mn(CO)_5Br$	CH_2Cl_2	RT	18	94

[a] RT = room temperature.

Spectroscopic studies indicate that in all of these complexes the $B_3H_8^-$ ligand is bound to the metal atom in a bidentate manner through bridging hydrogen atoms. Figure 1 shows the proposed structures of several of these complexes and the numbering system used in this study.

All but one of the metal octahydrotriborate derivatives that were obtained were the predicted products according to the reaction stoichiometry. In the case of the reaction of $B_3H_8^-$ with $(CO)_4FeBr_2$, in a 2:1 ratio, the expected product was a bis(octahydrotriborate) species, $(CO)_2Fe(B_3H_8)_2$. The actual product (formed at −30 °C) is $(H)(CO)_3FeB_3H_8$, which was obtained as an isomerically pure product. The relatively high yield (30%, estimate) of a stereospecific product suggests that a facile multistep selective pathway (or a nonspecific pathway involving isomers of greatly different stabilities) is responsible for the observed product. Though plausible formulations for the precursor(s) to $(H)(CO)_3FeB_3H_8$ are uncertain, formation of a bis(octahydrotriborate)–iron carbonyl complex and its subsequent decomposition to the observed product would at least provide a mechanism through which a hydride could become incorporated into the molecule. Equally elusive is the

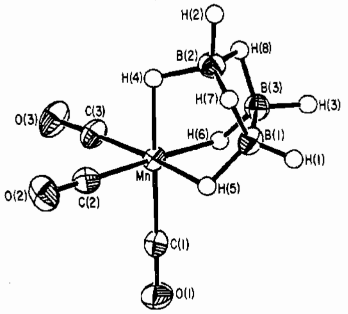

Figure 2. The static molecular structure of (CO)$_3$MnB$_3$H$_8$.

mechanism by which the decomposition of (H)(CO)$_3$FeB$_3$H$_8$ leads to the formation of the thermodynamically favored product, 1-(CO)$_3$FeB$_4$H$_8$.[5] The thermal decomposition of a sample of pure (H)(CO)$_3$FeB$_3$H$_8$ in methylene chloride solution at room temperature produces CO, H$_2$, 1-(CO)$_3$FeB$_4$H$_8$, B$_2$H$_6$, and B$_4$H$_{10}$ as the major products.

Preparation of (CO)$_4$MnB$_3$H$_7$X [X = Halogen]. Reactions between equimolar quantities of elemental halogens and (CO)$_4$MnB$_3$H$_8$ in methylene chloride solution in vacuo produce monohalogenated products.

$$(CO)_4MnB_3H_8 + X_2 \rightarrow (CO)_4MnB_3H_7X + HX$$

When X$_2$ = Br$_2$ the yields of HBr and (CO)$_4$MnB$_3$H$_7$Br are nearly quantitative. When X$_2$ = Cl$_2$ the yield of HCl is quantitative but yields of (CO)$_4$MnB$_3$H$_7$Cl are only on the order of 10–20% due to difficulties encountered during the purification (significant product decomposition accompanies purification). For X$_2$ = I$_2$ the course of the reaction is complex and different from the chlorine and bromine reactions and is characterized by the evolution of large quantities of noncondensable gases. The desired product, (CO)$_4$MnB$_3$H$_7$I, is obtained in yields of less than 1%.

Halogenation of (CO)$_4$MnB$_3$H$_8$ occurs at the unique boron atom, B(2), and may be stereospecific (vide infra). Figure 1c shows one of the two possible geometrical isomers for the (CO)$_4$MnB$_3$H$_7$X molecule.

Preparation of (CO)$_3$MnB$_3$H$_8$. Tricarbonyl[octahydrotriborato(1−)]manganese, (CO)$_3$MnB$_3$H$_8$, is prepared by the photolytic or thermal decarbonylation of (CO)$_4$MnB$_3$H$_8$.

$$(CO)_4MnB_3H_8 \xrightarrow[\text{or } 180\ ^\circ C]{UV} (CO)_3MnB_3H_8 + CO$$

The reaction is driven to completion by the constant removal of carbon monoxide from the system. The pure product, (CO)$_3$MnB$_3$H$_8$, is a yellow-orange liquid at room temperature and is obtained in approximately 80% yield. The solid-state structure of (CO)$_3$MnB$_3$H$_8$ has been determined by a single-crystal x-ray diffraction study[6] to be that shown in Figure 2.

The decarbonylation of (CO)$_4$MnB$_3$H$_8$ is thought to proceed with the loss of the axial carbon monoxide ligand, as is stereodynamically required if the bidentate B$_3$H$_8^-$ ligand folds over and bonds to the metal atom through hydrogen atom H(4), thereby completing the conversion of the ligand to tridentate functionality. This is certainly the simplest mechanism and requires minimal atom movement. In support of this proposed mechanism, the axial Cr–C bond length in [(CO)$_4$CrB$_3$H$_8$]$^-$ is 1.900 (10) Å whereas the equatorial bond length is 1.824 (7) Å. Guggenberger[2c] attributes the shorter equatorial Cr–C bond length to increased π back-donation from the metal to these carbonyl ligands. The result is an axial Cr–C bond which is weaker than the equatorial Cr–C bond. Therefore, since [(CO)$_4$CrB$_3$H$_8^-$][2c] and (CO)$_4$MnB$_3$H$_8$ are isostructural and isoelectronic, one would predict that the axial carbonyl ligand should be easier to remove from the (CO)$_4$MnB$_3$H$_8$ molecule. There is no ready explanation for the observation that (CO)$_4$MnB$_3$H$_8$ is the only metal complex of the bidentate B$_3$H$_8^-$ ligand which has been shown to undergo decarbonylation to a metal complex of the tridentate B$_3$H$_8^-$ ligand.

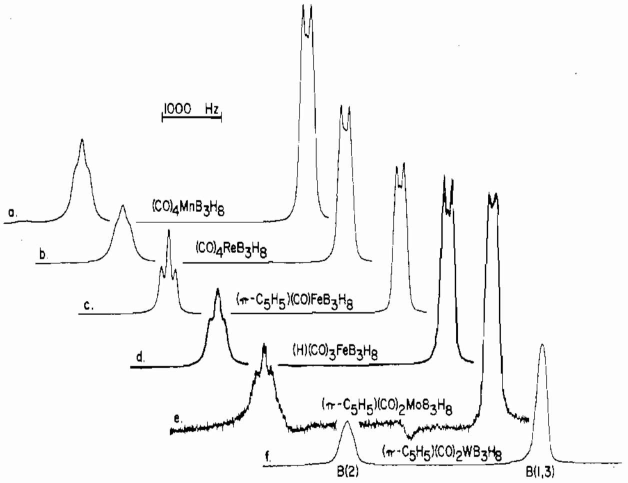

Figure 3. ^{11}B NMR spectra (86.65 MHz) of selected bidentate B$_3$H$_8^-$ metal complexes.

Reactions of (CO)$_3$MnB$_3$H$_8$. The reaction between (CO)$_3$MnB$_3$H$_8$ and excess carbon monoxide in CH$_2$Cl$_2$ solvent at room temperature produces (CO)$_4$MnB$_3$H$_8$ in approximately 95% yield, thereby establishing the equilibrium

$$(CO)_4MnB_3H_8 \underset{\sim 95\%}{\overset{UV \text{ or } \Delta,\ >80\%}{\rightleftarrows}} (CO)_3MnB_3H_8 + CO$$

This reaction represents the only known case of reversible bidentate–tridentate behavior for a borane ligand.[7]

Nearly quantitative reactions also result when (CO)$_3$MnB$_3$H$_8$ is mixed with an equimolar quantity of PF$_3$ or NH$_3$ in CH$_2$Cl$_2$ solvent.

$$(CO)_3MnB_3H_8 + L \xrightarrow{CH_2Cl_2} (L)(CO)_3MnB_3H_8$$
$$L = PF_3, NH_3$$

In both cases the octahedral coordination of the metal atom is retained by conversion from tridentate to bidentate B$_3$H$_8^-$ functionality coupled with addition of the PF$_3$ or NH$_3$. NMR and infrared analyses of the products confirm the bidentate B$_3$H$_8^-$ functionality but also indicate that the products are formed as a mixture of isomers.

In the predicted *fac* isomer, the ligand L would occupy an axial position vacated by scission of, for example, the Mn–H(4) bond. The presence of other isomers suggests that other more complex mechanisms are also operable.

NMR Studies of Static M–B$_3$H$_8$ Complexes. (a) (CO)$_4$MnB$_3$H$_8$, (CO)$_4$ReB$_3$H$_8$, (η^5-C$_5$H$_5$)(CO)FeB$_3$H$_8$, (η^5-C$_5$H$_5$)(CO)$_2$MoB$_3$H$_8$, and (η^5-C$_5$H$_5$)(CO)$_2$WB$_3$H$_8$. The normal ^{11}B spectra of these complexes (Figure 3 and Table II) consist of a low-field triplet of area 1 and a high-field "doublet" resonance of area 2 which contains couplings in addition to the major doublet coupling. This is shown by selectively decoupling the M–H–B protons and observing that the high-field grouping becomes a more well-resolved "doublet", although it is still broad, indicating that additional couplings are present. Upon broad-band ^{1}H decoupling the resonance collapses to a sharp singlet, indicating that its complexity is due exclusively to ^{1}H–^{11}B coupling.

Figure 4 shows the line-narrowed ^{11}B NMR spectra of the high-field group under a variety of selective decoupling conditions which, when line narrowed,[8] reveal a wealth of previously unresolved fine structure. Short-range major

Table II. ^{11}B NMR Data for Bidentate B_3H_8 and B_3H_7X Complexes[a]

			Chemical shift[b] [coupling constant][c]	
Complex	Solvent	Temp, °C	B(1,3)	B(2)
$(CO)_4MnB_3H_8$	$(C_2H_5)_2O$	Ambient to −40	−42.2 [133]	+1.5 [123]
	C_6D_6	Ambient	−41.8 [134]	+2.4
	CD_2Cl_2	Ambient	−41.9 [134, 140*]	+2.4
	CD_2Cl_2	−36.2	−41.8 [127, 139*]	+1.9
$(CO)_4ReB_3H_8$	C_6D_6	Ambient	−43.3 [142]	+0.3
	CD_2Cl_2	Ambient	−43.2 [132]	+0.3
$(\eta^5\text{-}C_5H_5)(CO)FeB_3H_8$	C_6D_6	Ambient	−42.0 [132]	+3.4 [122]
	CD_2Cl_2	Ambient	−42.5 [127, 139*]	+2.5 [125]
$(H)(CO)_3FeB_3H_8$	CD_2Cl_2	Ambient	−42.1 [127]	+3.0 [127]
	CD_2Cl_2	−36.2	−42.0 [137, 142*]	+2.8 [107]
$(\eta^5\text{-}C_5H_5)(CO)_2MoB_3H_8$	C_6D_6	Ambient	−40.7 [98, 128*]	+4.0 [112]
$(\eta^5\text{-}C_5H_5)(CO)_2WB_3H_8$	$(CD_3)_2CO$	Ambient	−42.5	−4.3
$(Ph_3P)(CO)_3MnB_3H_8$[d]	C_6D_6	Ambient	−38.5, −39.9	+1.4
	CD_2Cl_2	Ambient	−38.3, −40.6	+0.3
$(Ph_2PCH_2CH_2PPh_2)(CO)_2MnB_3H_8$	C_6D_6/DMF	Ambient	−40.6	+3.8
$(PF_3)(CO)_3MnB_3H_8$[d]	C_6D_6	23	−41.6, −42.8	+3.2, +2.2
	$CD_3C_6D_5$	23	−41.6, −42.8	+2.6
$(NH_3)(CO)_3MnB_3H_8$[d]	C_6D_6	23	−39.2, −40.3	+0.2
	CD_2Cl_2	23	−39.2, −40.2	−0.2
$(CO)_4MnB_3H_7Cl$	CD_2Cl_2	−36.2	−41.3 [122, 139*]	+9.0 [122, 139*]
	CD_2Cl_2	+23	−41.3 [42*]	+9.4
$(CO)_4MnB_3H_7Br$	CD_2Cl_2	−36.2	−41.6 [137*]	+2.3 [98]
	CD_2Cl_2	+23	−41.6 [44]	+2.5
	$CD_3C_6D_5$	+23	−41.9	+2.7
$(CO)_4MnB_3H_7I$	CD_3CN	+23	−41.1	−11.2

[a] All reported values were obtained at 86.653 MHz. [b] Chemical shifts are expressed in ppm relative to $BF_3 \cdot O(C_2H_5)_2 = 0$. Downfield shifts are positive.[16] [c] Coupling constants, in Hz, were obtained from the normal ^{11}B NMR spectra, except for starred (*) values, which were obtained from the line-narrowed normal spectra. [d] These samples were composed of a mixture of isomers.

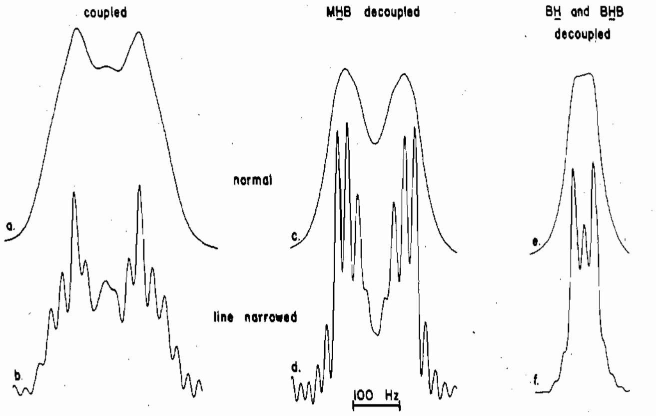

Figure 4. ^{11}B NMR spectra (86.65 MHz) of the B(1,3) resonance of $(CO)_4MnB_3H_8$ in $CDCl_2$ at +23 °C.

couplings include ^{11}B(1)–H(1), –H(5), and –H(7), and the ^{11}B(3) counterparts. Long-range couplings may include ^{11}B(1)–H(3), –H(6), –H(8), –H(2), and –H(4), and the ^{11}B(3) counterparts. In addition to these couplings the exact appearance of the line-narrowed spectrum will depend on the limiting line widths, the solvent, the temperature (e.g., thermal decoupling phenomena, etc.), the phasing of the spectrum, and the severity of the data manipulation. The appearance of the spectra that have been simultaneously line-narrowed and decoupled will also depend upon the decoupling frequency and power. Thus, care must be taken in analyzing line-narrowed spectra, and only the major features of most line-narrowed spectra can be interpreted with certainty.

The line-narrowed spectra of the high-field group of several bidentate octahydrotriborate complexes exhibit a striking similarity, which suggests that there is little direct interaction of the metal atom with B(1,3). The line-narrowed ^{11}B spectrum of the high-field grouping of 98% ^{11}B enriched B_4H_{10}[8] is very similar to the patterns reported here (Figure 4b). Our conclusions regarding the interpretation of these couplings are in agreement with those reported for B_4H_{10}.[8]

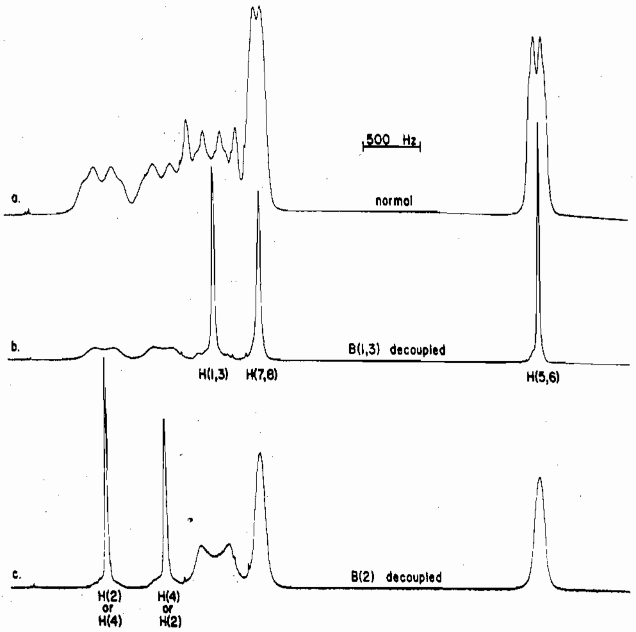

Figure 5. ^{1}H NMR spectra (270 MHz) of $(CO)_4ReB_3H_8$ in $CDCl_2$ at +23 °C.

Line narrowing enhances the resolution of the low-field triplet in these ^{11}B NMR spectra, but no additional fine structure is observed. This indicates nearly identical coupling constants $J_{B(2)-H(2)}$ and $J_{B(2)-H(4)}$ and small coupling constants to the adjacent bridge hydrogen atoms.

The ^{1}H NMR spectra indicate the presence of five distinct hydrogen environments for the $B_3H_8^-$ protons in these static bidentate complexes (Figure 5). The two resonances at lowest field, H(2) and H(4), correspond to the terminal hydrogens on the unique boron atom, B(2). It is not possible to establish specifically which resonance is due to H(2) and which is due

Table III. ^{1}H NMR Data for Bidentate B_3H_8 Complexes[a]

Complex	Solvent	Temp, °C	Chemical shift[b] [coupling constant][c]				
			H(1,3)	H(2), H(4)[e]	H(5,6)	H(7,8)	H(9)	Other
$(CO)_4MnB_3H_8$	C_6D_6	Ambient	1.03 [140]	2.74, 3.03	−12.05 [65]	−0.80 [58]		
	$CD_3C_6D_5$/ $(CD_3CD_2)_2O$	Ambient	0.93 [142]	2.65, 2.93	−12.06 [50]	−0.88 [55]		
	CD_2Cl_2	Ambient	0.88 [143]	2.69, 2.84	−11.86 [52]	−0.83 [53]		
	CD_2Cl_2	−45	0.81 [163]	2.63, 2.77	−11.89 [58]	−0.88 [47]		
$(CO)_4ReB_3H_8$	C_6D_6	Ambient	1.22 [147]	2.78 [153], 4.76 [156]	−9.33 [65]	−0.28 [53]		
	$CD_3C_6D_5$/ $(CD_3CD_2)_2O$	Ambient	1.13 [147]	2.72 [151], 4.62 [157]	−9.29 [63]	−0.34 [57]		
	CD_2Cl_2	Ambient	1.17 [150]	2.86 [142], 4.60 [150]	−8.97 [65]	−0.17 [57]		
$(\eta^5\text{-}C_5H_5)(CO)FeB_3H_8$	C_6D_6	Ambient	1.19 [143]	2.28, 3.91	−15.81 [59]	−1.42 [56]		3.83 (C_5H_5)
	CD_2Cl_2	Ambient	0.74 [142]	1.67, 3.15 [132]	−15.76 [60]	−1.90 [54]		4.76 (C_5H_5)
	CD_2Cl_2	−45	0.65 [146]	1.58, 3.06 [148]	−12.56 [66]	−1.96 [56]		4.76 (C_5H_5)
$(H)(CO)_3FeB_3H_8$	CD_2Cl_2	Ambient	0.68 [135], 0.96 [138]	2.62, 2.95 [132]	−8.81 [59], −12.72 [56]	−0.80, −0.92	−10.66	
	CD_2Cl_2	−45	0.62 [133], 0.89 [141]	2.56, 2.88	−8.83 [69], −12.73 [61]	−0.82, −0.99	−10.65	
	$CD_3C_6D_5$	−45	0.92, 1.26	2.72, 3.43	−9.13 [71], −12.97 [49]	−0.72, −0.89	−11.25	
$(\eta^5\text{-}C_5H_5)(CO)_2MoB_3H_8$	C_6D_6	Ambient	1.38 [138]	2.92, 3.80	−10.36 [68]	−0.28 [62]		4.37 (C_5H_5)
$(\eta^5\text{-}C_5H_5)(CO)_2WB_3H_8$	$(CD_3)_2CO$	Ambient			−10.04 [65]			
$(Ph_3P)(CO)_3MnB_3H_8$[d]	C_6D_6	Ambient			−10.91	−0.60		6.96, 7.42 (Ph)
	CD_2Cl_2	Ambient			−11.20 [50]	−1.14		7.45 (Ph)
	CD_2Cl_2	−25			−11.24	−1.07		7.43 (Ph)
$(PF_3)(CO)_3MnB_3H_8$[d]	C_6D_6	23	1.13, 1.24	2.83, 3.14, 3.29	−0.63, −0.79	−11.83, −12.59		
$(NH_3)(CO)_3MnB_3H_8$[d]	CD_2Cl_2	23	0.29 [127]	2.74 [147]	−0.74	−9.55, −9.95		0.96 (NH_3)
	C_6D_6	23	0.32 [138]	3.16, 3.30 [147]	−0.51	9.83, −10.15		−0.86 (NH_3)
	$CD_3C_6D_5$	23		3.16 [149]	−0.46	−10.02, −10.26		−0.76 (NH_3)
	$CD_3C_6D_5$	−30	0.28	3.28	−0.53	−10.20		−1.04 (NH_3)

[a] All reported values were obtained at 270.071 MHz. [b] Chemical shifts are expressed in ppm (δ units) relative to $(CH_3)_4Si$. [c] Coupling constants, in Hz, are reported for the central members of the 1:1:1:1 quartets only. [d] These samples were composed of a mixture of isomers. [e] Absolute assignments to H(2) and H(4) are uncertain.

to H(4). The separation between these two resonances ranges from a maximum of approximately 2.0 ppm in $(CO)_4ReB_3H_8$ to a minimum of only 0.2 ppm in $(CO)_4MnB_3H_8$ (Table III). The terminal hydrogen atom resonances, H(1,3), on the boron atoms adjacent to the metal generally occur at about δ 1. The boron bound bridging hydrogens, BHB, absorb slightly upfield (δ 0 to −2) from Me_4Si. The MHB hydrogens are shifted far upfield (δ −9 to −16).[9] These BH, BHB, and MHB ^{1}H NMR resonances all collapse to sharp singlets upon ^{11}B decoupling, indicating the presence of C_s symmetry in $(CO)_4MnB_3H_8$, $(CO)_4ReB_3H_8$, $(\eta^5\text{-}C_5H_5)(CO)FeB_3H_8$, and $(\eta^5\text{-}C_5H_5)(CO)_2MoB_3H_8$.

(b) $(H)(CO)_3FeB_3H_8$. This molecule is a special case in that it appears to exist as a single isomer which lacks the plane of symmetry present in $(CO)_4MnB_3H_8$, $(CO)_4ReB_3H_8$, $(\eta^5\text{-}C_5H_5)(CO)FeB_3H_8$, and $(\eta^5\text{-}C_5H_5)(CO)_2MoB_3H_8$. The ^{1}H NMR spectra (Figure 6) of $(H)(CO)_3FeB_3H_8$ show that all nine protons in the molecule absorb at different frequencies. The sharp spike at δ −10.65 is the terminal hydrogen atom, H(9), on the iron atom. The area associated with the resonance for H(9) is small, as a result of saturation, when compared to the other resonances. Absolute assignments for the hydrogen atoms in the $B_3H_8^-$ fragment cannot be made with certainty, but probable assignments are indicated on Figure 6. The absence of the plane of symmetry in the $(H)(CO)_3FeB_3H_8$ molecule is not apparent from its ^{11}B NMR spectra (Figure 3d) which suggest that B(1) and B(3) are equivalent. Since the molecule appears to be static at all temperatures studied (−85 to +23 °C), the equivalence must be accidental.

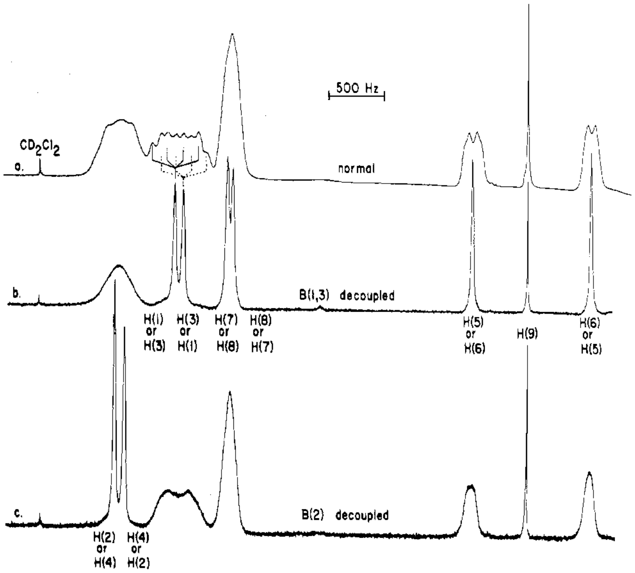

Figure 6. ^{1}H NMR spectra (270 MHz) of $(H)(CO)_3FeB_3H_8$ in CD_2Cl_2 at −45 °C.

Ideally one would expect the ^{1}H resonances for the terminal hydrogens on boron to be 1:1:1:1 quartets [$I(^{11}B) = {}^3/_2$]. In practice, however, the line shape of the resonance is often not a perfect quartet, as observed in the spectra presented here. The departure from ideality has been explained on the basis of an additional proton coupling to ^{10}B (20% abundance, $I = 3$, $J_{^1H-^{10}B} \sim 0.33 J_{^1H-^{11}B}$)[10] as well as a line-shape dependence on nuclear quadrupole effects.[11,12]

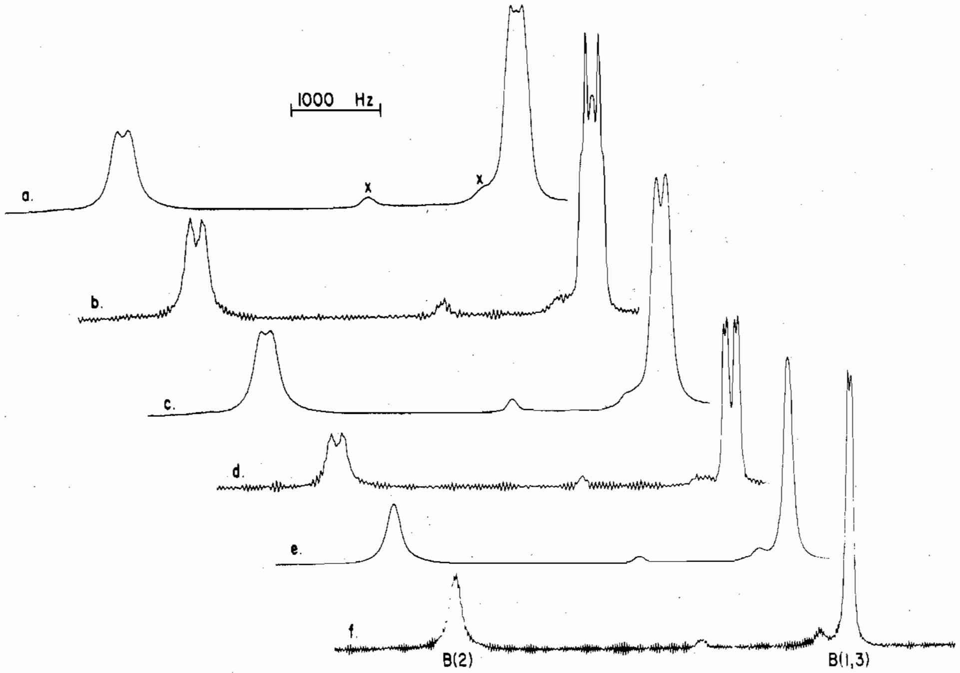

Figure 7. ^{11}B spectra (86.65 MHz) of $(CO)_4MnB_3H_7Cl$ in CD_2Cl_2 at −36 °C: a, normal; b, normal and line narrowed; c, M*H*B decoupled; d, M*H*B decoupled and line narrowed; e, B*H* and B*H*B decoupled; f, B*H* and B*H*B decoupled and line narrowed.

Tables II and III indicate only slight dependences of the appearance of the ^1H and ^{11}B NMR spectra on solvent and temperature for the complexes $(CO)_4MnB_3H_8$, $(CO)_4FeB_3H_8$, $(\eta^5\text{-}C_5H_5)(CO)FeB_3H_8$, and $(H)(CO)_3FeB_3H_8$. As a general rule the resolution of the ^1H and ^{11}B NMR spectra of these complexes is enhanced by increasing solvent polarity and increasing temperature. Thermal decoupling[13] and solution viscosity may in part account for the slight temperature dependence. The ^{11}B chemical shifts for a given complex appear to be independent of solvent and temperature. The same independence is observed for ^1H spectra, except in the case of $(\eta^5\text{-}C_5H_5)(CO)FeB_3H_8$, in which the chemical shift of the cyclopentadienyl hydrogens appears to be influenced by the solvent ($\delta = 4.76$ in CD_2Cl_2 vs. $\delta = 3.83$ in C_6D_6) but not by the temperature. The chemical shifts of H(1,3), H(2), H(4), and H(7,8) in $(\eta^5\text{-}C_5H_5)(CO)FeB_3H_8$ are also solvent dependent. The chemical shifts of the MHB hydrogen atoms, H(5,6), of $(\eta^5\text{-}C_5H_5)(CO)FeB_3H_8$ appear to be independent of solvent but dependent on temperature (in CD_2Cl_2: $\delta = -15.76$ at 23 °C vs. $\delta = -12.56$ at −45 ±5 °C). Only the four complexes mentioned, $(CO)_4MnB_3H_8$, $(CO)_4ReB_3H_8$, $(\eta^5\text{-}C_5H_5)(CO)FeB_3H_8$, and $(H)(CO)_3FeB_3H_8$, have been studied extensively with regard to these solvent and temperature effects.

(c) $[(C_6H_5)_3P](CO)_3MnB_3H_8$, $(NH_3)(CO)_3MnB_3H_8$, and $(PF_3)(CO)_3MnB_3H_8$. The NMR spectra of these complexes are consistent with the bidentate mode of attachment for the $B_3H_8^-$ ligand but are complicated by the fact that each exists as a mixture of isomers.

The normal ^{11}B NMR spectrum of $[(C_6H_5)_3P](CO)_3MnB_3H_8$ consists of a low-field grouping of area 1 and a high-field grouping of area 2. These resonances lack the fine structure visible in the metal–B_3H_8 derivatives discussed above, presumably a result of the presence of ^{31}P in the molecule. The ^1H-decoupled ^{11}B NMR spectra indicate the presence of two isomers. The ^1H NMR spectra are solvent dependent. In CD_2Cl_2, for example, all phenyl hydrogens appear nearly equivalent, but in C_6D_6 there are two distinct phenyl absorptions separated by almost 0.5 ppm. Specifically which isomers are responsible for the observed NMR spectra is uncertain. The starting organometallic material used was *trans*-$[(C_6H_5)_3P](CO)_4MnBr$. The isomers formed by simple attachment of bidentate $B_3H_8^-$ to this starting material would be the optical isomers, a and b, shown below. Internal rearrangement must be occurring during the synthesis, producing one or two geometrical isomers.

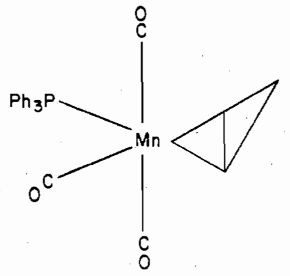

a

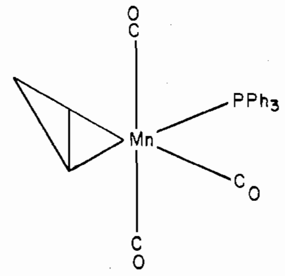

b

The ^{11}B NMR spectra of $(PF_3)(CO)_3MnB_3H_8$ and $(NH_3)(CO)_3MnB_3H_8$ are consistent with the ^{11}B NMR spectra of the static bidentate $B_3H_8^-$ metal complexes presented earlier. The ^1H NMR spectra of these PF_3 and NH_3 complexes show the molecules to be static and confirm that the $B_3H_8^-$ ligand is bound to the metal through bridging hydrogen atoms. Decoupled ^1H and ^{11}B NMR spectra exhibit more resonances than would be present for an isomerically pure product.

NMR Studies of Fluxional M–B_3H_8 Complexes. (a) $(CO)_4MnB_3H_7X$ (X = Br, Cl). The $(CO)_4MnB_3H_7Cl$ and $(CO)_4MnB_3H_7Br$ complexes exhibit almost identical spectral behavior. At low temperatures the ^1H and ^{11}B NMR spectra are consistent with a static structure in which the halogen atom occupies a terminal position on the unique boron atom, B(2). Figure 1c shows one of the two possible static structures for $(CO)_4MnB_3H_7X$. At higher temperatures the $(CO)_4MnB_3H_7X$ molecule displays partially fluxional behavior.

The normal ^{11}B NMR low-temperature spectrum (−36 °C), Figure 7, consists of a doublet of area 1, corresponding to B(2), and a high-field "doublet" of area 2 corresponding to B(1,3). Expanded views of the high-field grouping under conditions of selective decoupling and line narrowing are shown in Figure 8. When line narrowed, the normal spectrum of this grouping has an appearance nearly identical with the line-narrowed high-field resonances for the static bidentate $B_3H_8^-$ complexes

Table IV. ^{1}H NMR Data for $(CO)_4MnB_3H_7X^a$

Complex	Solvent	Temp, °C	Chemical shift^b [coupling constant]^c			
			H(1,3)	H(2)	H(4,5)	H(6,7)
$(CO)_4MnB_3H_7Cl$	CD_2Cl_2	−70.5	0.87	3.44	0.42	−11.68
	CD_2Cl_2	−39.8	0.88 [162]	3.47 [182]	0.42	−11.69 [56]
	CD_2Cl_2	−17.3	0.90	3.49 [179]	0.46	−11.68 [62]
	CD_2Cl_2	−3.4	0.90	3.51 [168]	0.49	−11.67 [65]
	CD_2Cl_2	+9.9				−11.68 [62]
	CD_2Cl_2	+23	←	0.90	→	−11.65 [62]
	CD_2Cl_2	+41.0	←	1.13	→	−11.65 [53]
	CD_2Cl_2	+60.2	←	1.29	→	−11.65
$(CO)_4MnB_3H_7Br$	CD_2Cl_2	−70.5		3.44	0.33	−11.48
	CD_2Cl_2	−35.2	1.00 [162]	3.48 [182]	0.36	−11.47 [49]
	$CD_3C_6D_5$	−30	1.14	3.35	0.19	−11.94
	CD_2Cl_2	−17.3		3.48 [166]	0.47	−11.47 [62]
	CD_2Cl_2	−3.4				−11.45 [66]
	CD_2Cl_2	+9.9	←	1.03	→	−11.46 [63]
	$CD_3C_6D_5$	+23	←	0.93	→	−11.85 [60]
	CD_2Cl_2	+23	←	1.21	→	−11.45 [66]
	CD_2Cl_2	+41.0	←	1.28	→	−11.44 [66]
	CD_2Cl_2	+60.2	←	1.30	→	−11.43
$(CO)_4MnB_3H_7I$	CD_3CN	+23				−11.23 [71]

[a] All reported values were obtained at 270.071 MHz. [b] Chemical shifts are expressed in ppm (δ units) relative to $(CH_3)_4Si$. [c] Coupling constants, in Hz, are reported for the central members of the 1:1:1:1 quartets only.

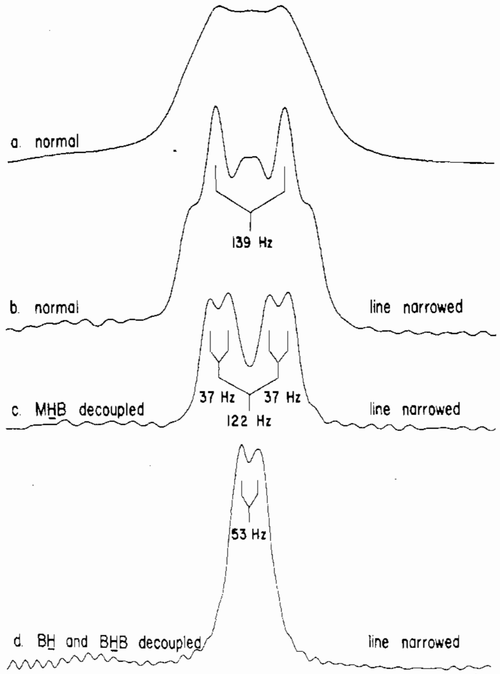

Figure 8. ^{11}B NMR spectra of the B(1,3) resonance of $(CO)_4MnB_3H_7Cl$ in CD_2Cl_2 at −36 °C.

discussed earlier (Figure 4b). When the hydrogen atoms bridging between the metal atom and the boron atoms adjacent to the metal atom are selectively decoupled, the high-field resonance doublet is revealed, the major coupling resulting from coupling to thermal hydrogen atoms, H(1,3), and the minor coupling resulting from the interaction of BHB hydrogens, H(4,5) with the B(1,3) nuclei. The low-field resonance remains a doublet (Figure 7c,d). When BH [H(1,2,3)] and BHB [H(4,5)] hydrogens are decoupled, both ^{11}B resonances appear to sharpen to singlets. Upon line narrowing, however, the low-field resonance remains a singlet but the high-field resonance proves to be a doublet, indicating coupling of B(1) and B(3) to the MHB hydrogen atoms.

Further evidence that halogen substitution occurs at B(2) in $(CO)_4MnB_3H_7X$ is provided by the observation that upon substitution the B(2) resonance is considerably shifted in the ^{11}B NMR spectrum when compared to the parent molecule, $(CO)_4MnB_3H_8$, but the B(1,3) resonance is not significantly shifted (Table II). The magnitude and direction of the ^{11}B chemical shifts of B(2) in $(CO)_4MnB_3H_7X$ relative to B(2) in $(CO)_4MnB_3H_8$ are similar to those observed for substiuted chloro, bromo, and iodo derivatives of pentaborane(9).[14] Table II lists the ^{11}B NMR data on the $(CO)_4MnB_3H_7X$ complexes as a function of temperature and solvent.

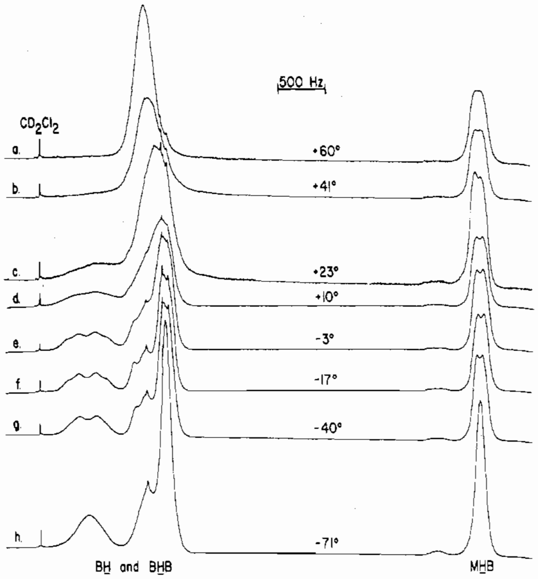

Figure 9. The temperature-dependent ^{1}H NMR spectra (270 MHz) of $(CO)_4MnB_3H_7Cl$ in CD_2Cl_2.

The low-temperature (−35.2 °C) ^{1}H NMR spectra of $(CO)_4MnB_3H_7Br$ indicate the presence of four distinct hydrogen environments in the molecule: (1) a resonance at very high field (area 2) δ −11.47 assigned to the MHB hydrogen atoms; (2) a broad structureless resonance at δ 0.36 (area 2) assigned to the BHB hydrogen atoms; (3) a resonance at δ 1.00 (area 2) assigned to terminal hydrogen atoms H(1) and H(3); and (4) a resonance at δ 3.48 (area 1) assigned to the single terminal hydrogen atom on B(2). The changes in the chemical shifts of the various proton environments upon substitution of a halogen atom for a hydrogen atom in the $(CO)_4MnB_3H_8$ molecule are tabulated in Table III. As expected, the largest shift changes occur for those hydrogen atoms bonded to the halogenated boron atom B(2). The temperature dependence of the ^{1}H NMR spectra of $(CO)_3MnB_3H_7Cl$ is shown in

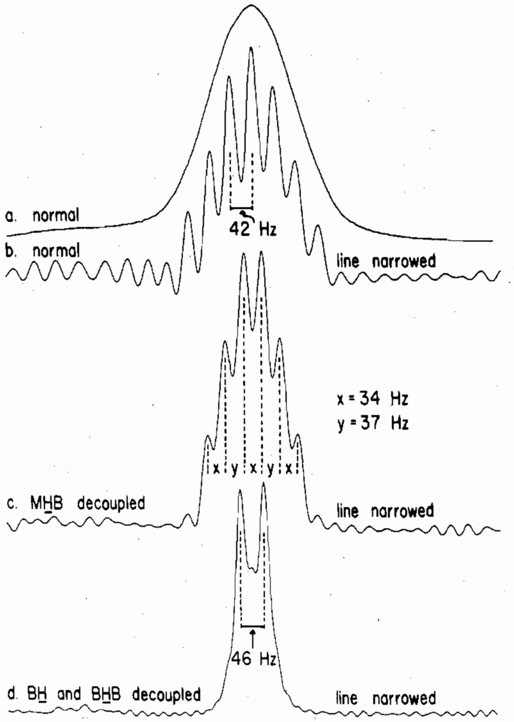

Figure 10. ^{11}B NMR spectra of the B(1,3) resonance of $(CO)_4MnB_3H_7Cl$ in CD_2Cl_2 at +23 °C.

Figure 9. Upon warming, solutions of $(CO)_4MnB_3H_7Br$ first show signs of departure from the static structure at about −20 °C, whereas solutions of $(CO)_4MnB_3H_7Cl$ do not exhibit any spectral changes until approximately −5 °C. As the temperature is raised above these static structure limits, the nature of the temperature dependence becomes apparent. The resonances due to H(1,3), H(2), and H(4,5) begin to lose their fine structure, merge, and finally coalesce to a single resonance at the weighted average position. The equivalence of these five hydrogens is further indicated by the collapse of this broad resonance to a singlet when ^{11}B is decoupled. The resonance assigned to the MHB hydrogens, H(6,7), is not temperature dependent (although a slight loss of resolution is noted at higher temperatures), which suggests that these hydrogen atoms are static. This selective exchange of hydrogens on the halogen-substituted B_3 triangular framework is particularly novel when compared to the static configuration of the unsubstituted $L_4MB_3H_8$ complexes and to the total equilibration of H and B environments in the free $B_3H_8^-$ anion.[15] In both the static and fluxional cases there is little doubt that the halogen atom is located in only one of the available terminal positions on B(2).[16]

The room temperature ^{11}B NMR spectra of $(CO)_4MnB_3H_7Cl$ and $(CO)_4MnB_3H_7Br$ corroborate the mode of fluxional behavior deduced from the ^1H NMR spectra. The ^{11}B NMR spectra of these complexes at ambient temperature (+23 °C) are nearly identical. Figure 10 shows expansions of the high-field grouping in the normal, decoupled, and line-narrowed ^{11}B spectra of $(CO)_4MnB_3H_7Cl$. The selectively decoupled ^{11}B spectra show that, with H(1) through H(5) decoupled, the line-narrowed spectrum of the high-field grouping is primarily a doublet, which indicates that the MHB protons are static on the NMR time scale. The line-narrowed high-field resonance, with the MHB hydrogens decoupled, is a sextet indicating that B(1,3) is coupled to five equivalent hydrogens [H(1) through H(5)]. The seven-line pattern exhibited in the normal line-narrowed ^{11}B NMR spectrum can thus be constructed from a doublet of sextets, the couplings arising from the interactions indicated above. The intensities of the individual members of these multiplets are not ideal, but the inherent parameters in the line-narrowing experiment can give rise to such apparent discrepancies, as can underlying couplings (e.g., $^{11}B-^{10}B$) that are not resolved but which contribute to line widths and peak intensities. The ^1H NMR resonance for the BH and BHB hydrogen atoms continues to narrow as the temperature is raised above room temperature, which indicates that the BH and BHB hydrogens are not exchanging in the fast-exchange limit at room temperature. Under these intermediate exchange conditions (i.e., room temperature) ideal line shapes for the ^{11}B NMR spectra are not expected. The major couplings present in the line-narrowed ^{11}B NMR spectra at room temperature do, however, support the variable-temperature ^1H NMR spectra.

Table V. NMR Data for $(CO)_3MnB_3H_8$

		Chemical shift [coupling constant, Hz]		
		$^1H^a$		$^{11}B^b$
Solvent	Temp, °C	H(1,2,3,7,8)	H(4,5,6)	B(1,2,3)
CD_2Cl_2	23	0.22	−11.06	−47.2
CD_2Cl_2	−49	0.10	−11.19 [99]	
C_6D_6	23	−0.02	−11.41	
$CD_3C_6D_5$	−30	−0.07	−11.45 [88]	
$CD_3C_6D_5$	−81	−0.19	−11.60	

[a] Chemical shifts are expressed in ppm (δ units) relative to $(CH_3)_4Si$. [b] Chemical shifts are expressed in ppm relative to $BF_3\cdot O(C_2H_5)_2$; downfield shifts are positive.[17]

The normal room temperature ^{11}B spectrum of the B(2) resonance should be a sextet resulting from coupling to five equivalent hydrogen atoms [H(1) through H(5)], but even when line narrowing is applied, this fine structure, if present, is not resolvable. A possible explanation for this is broadening by coupling to the halogen atom (^{35}Cl, ^{37}Cl, ^{79}Br, and ^{81}Br all have $I = 3/2$).

(b) $(CO)_3MnB_3H_8$. The static molecular configuration of $(CO)_3MnB_3H_8$ is shown in Figure 2.[6] The *fac*-$B_3H_8^-$ ligand is bound to the metal atom through three bridging hydrogen atoms, one to each of the three boron atoms. Each boron atom also has a single terminal hydrogen atom bonded to it. The other two hydrogen atoms in the molecule bridge between boron atoms. The resulting static molecular symmetry is C_{2v}. The ^1H and ^{11}B NMR spectra of solutions of $(CO)_3MnB_3H_8$ exhibit partially fluxional behavior on the NMR time scale, at temperatures as low as −80 °C.

The ^{11}B NMR spectrum of $(CO)_3MnB_3H_8$ consists of a single resonance (δ −47.2 ppm[17] CD_2Cl_2 solvent) which is temperature dependent. Unresolved fine structure, noted at about 0 °C, decreases as the temperature is raised or lowered. Upon decoupling ^1H a single very narrow resonance is observed, indicating the equivalence of the three boron environments.

The room temperature ^1H NMR spectrum of $(CO)_3MnB_3H_8$ consists of a broad signal of area 5 at δ −0.1 (vs. Me_4Si) and a somewhat narrower signal of area 3 at δ −11.5. Decoupling ^{11}B results in the narrowing of these two broad resonances to sharp singlets. The presence of three protons far upfield from tetramethylsilane suggests that the $B_3H_8^-$ ion is bound to the metal through three Mn–H–B bridge hydrogen bonds. The presence of a single resonance at lower field implies that the hydrogens that are not involved in Mn–H–B bridge bonding are equivalent, most likely as a result of rapid intramolecular exchange (on the NMR time scale) around the periphery of the B_3 triangle. Such exchange would also render the three boron atoms magnetically equivalent, as observed in the ^{11}B NMR spectra. At room temperature the low-field ^1H resonance [associated with H(1), H(2), H(3), H(7), and H(8)] exhibits poorly resolved fine structure. If the mode of fluxional behavior described above is in operation, one would expect to see a decet resonance. The fine structure disappears

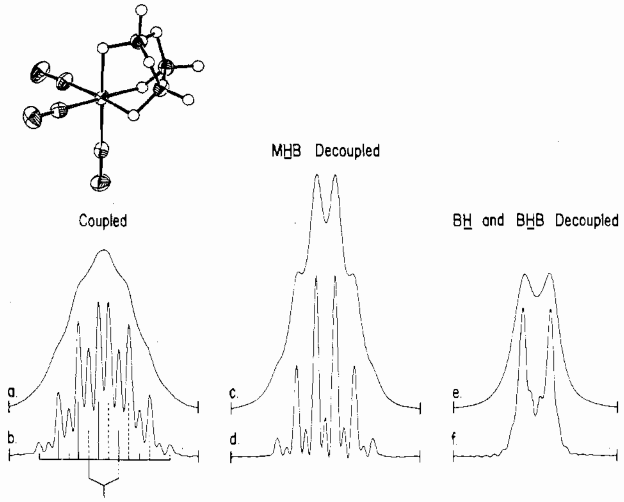

Figure 11. ^{11}B spectra (86.65 MHz) of $(CO)_3MnB_3H_8$ at −10 °C: a, normal fully coupled spectrum; b, same as a, but line narrowed; c, M*H*B decoupled; d, same as c, but line narrowed; e, B*H* and B*H*B decoupled; f, same as e, but line narrowed.

as the temperature is lowered but otherwise the spectrum remains essentially unchanged down to −81 °C, indicating that intramolecular exchange is still rapid at this temperature.

Line-narrowed ^{11}B NMR spectra with selective decoupling lend further support to the proposed fluxional behavior outlined above (Figure 11). When the boron-bound hydrogens [H(1), H(2), H(3), H(7), and H(8)] are decoupled, the ^{11}B resonance simplifies to a doublet, indicating that each boron atom is coupled to a single hydrogen atom that bridges to the manganese atom. When the Mn–H–B bridging hydrogen atoms [H(4), H(5), and H(6)] are selectively decoupled, the ^{11}B NMR assumes a sextet structure, indicating that five equivalent hydrogen atoms are spin coupled to the boron atoms. The normal line-narrowed spectrum can thus be constructed from a doublet ($J \approx 68$ Hz) of sextets ($J \approx 44$ Hz). In all of these line-narrowed spectra additional inexplicable fine structure is present, but the major couplings are consistent with the proposed mode of fluxional behavior.

The NMR spectra of $(CO)_3MnB_3H_8$ are consistent with a partially, or selectively, nonrigid molecule in which the hydrogen atoms bridging to the metal are static and the boron-bound hydrogen atoms are undergoing rapid internal exchange on the NMR time scale. The mechanism for hydrogen exchange in the constrained $(CO)_3MnB_3H_8$ framework is undoubtedly somewhat different from that in free $B_3H_8^-$ anion[18] as only one side of the B_3 unit is available in the complex. On the other hand the slightly higher exchange barrier observed for $(CO)_4MnB_3H_7X$ implies yet another mechanistic variation that probably becomes accessible as a result of the presence of the electron-rich halogen.

Experimental Section

Diethyl ether, tetrahydrofuran, toluene, benzene, and heptane were distilled in vacuo at room temperature from lithium aluminum hydride immediately prior to use. When large quantities (greater than 100 mL) of rigorously dry solvents were needed, they were distilled under nitrogen at atmospheric pressure. Diglyme and benzene were distilled from sodium metal, and tetrahydrofuran was distilled from benzophenone ketyl. Methylene chloride was dried and stored over 3 Å molecular sieves. Deuterated NMR solvents were dried in the same manner as their protonic counterparts. Chromatography solvents were reagent grade and were deaereated prior to use. NaB_3H_8 was prepared by a previously described method[19] but modified in that the diborane was generated [from $BF_3{\cdot}O(C_2H_5)_2 + NaBH_4$] in a separate reaction pot and then bubbled into another reaction flask containing $NaBH_4$ in diglyme at 105 °C. The tetramethylammonium,[20] cesium,[19] and thallium[21] octahydrotriborate salts were then prepared by metathesis from NaB_3H_8. All gas- and solution-phase infrared spectra were obtained in cells with NaCl windows. The low-temperature infrared spectra were obtained by coating a thin film of the metalloborane complex on a 1 mm thick IRTRAN2 (ZnS) window in vacuo at −196 °C. Ultraviolet irradiation sources used either an ordinary General Electric Mercury Projector Spot (No. H100PSP444) or a 450-W photochemical immersion lamp (No. 6515-34) and its complementary quartz immersion well (No. 6515-25), from Ace Glass, Inc.

Low-resolution (±10 cm^{-1}) infrared spectra were obtained on a Perkin-Elmer Model 700 infrared spectrophotometer. High-resolution (±2 cm^{-1}) infrared spectra were obtained on a Digilab FTS-20 spectrophotometer.

NMR spectra were obtained on Varian XL-100-15 or Bruker WH-270 spectrometers. The Varian instrument operates at 100.1 MHz (^1H) and 32.1 MHz (^{11}B) and is interfaced with a Varian 620/L minicomputer. The Bruker instrument operates at 270.071 MHz (^1H) and 86.653 MHz (^{11}B) and is controlled by a Nicolet Instruments Model 1080 computer. Both instruments are equipped with commercially available low-temperature accessories.[22] Mass spectra were obtained on an AEI-MS9 mass spectrometer.[22]

General Synthetic Procedures. Due to the air sensitivity of the products obtained, standard high-vacuum and inert-atmosphere techniques were employed throughout these syntheses.[23] Unless otherwise specified all reactions were carried out in vacuo in Pyrex reaction flasks equipped with a high-vacuum Teflon stopcock. For reactions requiring ultraviolet irradiation, flasks with quartz bulbs were generally used.

The octahydrotriborate source can be either covalent [$(CH_3)_2AlB_3H_8$[3] and $(CH_3)_2GaB_3H_8$[3]] or ionic [$M^+B_3H_8^-$]. Due to the limited solubility of the ionic $B_3H_8^-$ salts in the solvents employed, the rate of reaction was enhanced by grinding the salt in a mortar prior to introducing it into the reaction flask. The addition of about twenty-five 4-mm borosilicate glass beads ensured the production of fresh reaction surfaces on the octahydrotriborate salt as the reaction proceeded.

The reaction flask was charged with the organometallic reagent, a Teflon-coated magnetic stirring bar, glass beads, and, usually, about 30% excess of the triborohydride salt. The flask was attached to the vacuum line and evacuated. The solid reagents were dried by evacuation for at least 15 min (only minor losses of volatile organometallics occurred). The reaction flask was then immersed in liquid nitrogen and the solvent distilled in vacuo into the flask. If the octahydrotriborate source was $(CH_3)_2AlB_3H_8$ or $(CH_3)_2GaB_3H_8$, it was distilled into the flask at this time. The reaction flask valve was closed and the reactant mixture allowed to warm to the desired reaction temperature while stirred magnetically. Temperatures below room temperature were maintained by immersion of the reaction pot in an appropriate cooling bath. Since carbon monoxide is evolved in each of these reactions, the progress of the reaction can easily be monitored by freezing the reaction vessel in liquid nitrogen and observing the CO pressure (vapor pressure of CO = 400 Torr at −196 °C). The CO was pumped away, the flask valve closed, and the reaction continued at the desired temperature.

After the reaction was complete, the volatile reaction products were transferred to the vacuum line and separated by trap-to-trap fractionations. The products remaining in the reaction flask were worked up using Schlenk, glovebag, and other inert-atmosphere techniques. The residues from all of these reactions are often pyrophoric in air. The specifics of the individual preparations and reactions are described below.

$(CO)_4MnB_3H_8$. Tetracarbonyl[octahydrotriborato(1−)]manganese, $(CO)_4MnB_3H_8$, can be prepared from a variety of starting reagents, as summarized in Table I. Method (1) is much preferred to method (2).

(1) $B_3H_8^-$ Salts + $Mn(CO)_5X$. Cesium, thallium, and tetramethylammonium salts of $B_3H_8^-$ all gave high yields of $(CO)_4MnB_3H_8$. In a typical preparation 13 mmol of $(CH_3)_4NB_3H_8$ with 10 mmol of $Mn(CO)_5Br$[24] at room temperature in ~40 mL of CH_2Cl_2 produced at 70% yield of the product in 60 h. The $(CO)_4MnB_3H_8$ is purified on the vacuum line by distillation through a 0 °C U-trap and condensation in a −36 °C U-trap.

Larger scale preparations (up to 100 mmol) have been carried out under inert-atmosphere conditions in a hood using the appropriate scale-up in reactant and solvent quantities. The reaction is complete in about 72 h when the reaction vessel is slowly purged with N_2. The bulk of the solvent can be removed at or below room temperature under reduced pressure on the bench. Heating should be avoided as it leads

Table VI. Infrared Absorption Frequencies (cm^{-1})[a]

$(CO)_4MnB_3H_8$	Gas phase, ~1 Torr: 2560 m, 2550 m, sh, 2500 mw, 2210 w, 2150 m, 2070 s, 2010 s. 1980 w, sh, 1825 w, 865 vw
	Thin film at −196 °C: 2530 vs, 2480 s, 2430 vw, 2205 s, 2150 s, 2015 vs, 1830 s, 1485 mw, 1435 mw, 1295 mw, 1210 ms, 1165 ms, 1055 m, 1010 ms, 990 ms, 970 ms, 955 m, 915 ms, 880 s, 860 s, 830 s, 770 vw, 700 s
	Gas phase, ~1 Torr, ±2 cm^{-1}: 2563 w, sh, 2558 m, sh, 2551 s, sh, 2546 m, 2541 s, sh, 2531 mw, 2525 mw, 2484 s, sh, 2479 mw, 2182 w, 2128 m, 2083 vw, 2078 w, 2060 s, 2044 s, 2019 s, 2014 s, 1980 w, 1823 w, 1278 vw, 1199 w, 1158 w, 1000 vw, 965 vw, 906 vw, 871 m, sh, 855 w, 833 w
$(CO)_4ReB_3H_8$	Gas phase, saturated vapor (~0.5 Torr): 2575 w, 2505 vw, 2170 w, 2070 ms, 2010 m
	Thin film at −196 °C: 2545 s, 2485 s, 2190 ms, 2150 s, 1995 vs, 1800 vw, br, 1530 mw, 1320 vw, 1295 w, 1225 m, 1200 w, sh, 1160 m, 1105 vw, 1070 mw, 1015 m, 990 m, 965 m, 910 ms, 855 ms, 800 vw, 760 m, sh, 750 vw, 695 m
$(\eta^5\text{-}C_5H_5)(CO)FeB_3H_8$	CH_2Cl_2 solution (1800–2800-cm^{-1} region only): 2525 ms, 2460 m, 2190 m, 1995 s, 1870 vw, br
	KBr mull: 3120 m, 2505 s, 2460 s, 2390 m, sh, 2350 m, sh, 2300 w, sh, 2165 s, 1980 vs, 1940 s, sh, 1865 m, sh, br, 1800 w, sh, br, 1705 m, 1530 m, 1430 ms, 1215 m, sh, 1170 m, 1040 m, 990 s, 950 ms, 910 m, 885 w, sh, 850 s, 830 s, sh, 810 m, sh
$(H)(CO)_3FeB_3H_8$	Thin film at −196 °C: 2540 m, 2485 m, 2330 w, 2210 mw, 2145 ms, 2060 s, 2020 w, sh, 1915 w, 1835 mw, 1220 w, 1160 w, 1055 w, 1010 w, 975 w, 955 vw, 925 w, 880 mw, 835 mw, 810 w, 775 m, 740 m, 695 m
$(Ph_3P)(CO)_3MnB_3H_8$*	CH_2Cl_2 solution: 2545 w, 2520 m, sh, 2485 w, 2185 vw, 2055 ms, 1970 ms, 1945 ms, 1870 vw, 1490 w, 1440 mw, 1100 w
	KBr mull: 3095 s, sh, 3070 w, 3030 w, sh, 2550 mw, 2515 m, 2465 m, 2170 w, 2125 vw, 2050 s, 1985 ms, 1970 s, 1960 m, 1920 s, 1905 m, sh, 1870 vw, 1485 mw, 1435 m, 1425 w, sh, 1400 vw, 1335 vw, 1320 vw, 1285 vw, br, 1190 w, 1165 vw, 1100 m, sh, 1095 mw, 1080 vw, 1055 vw, 1035 vw, 1000 w, 975 vw, 940 w, sh, 905 w, 895 m, sh, 860 vw, 835 vw, 745 mw, 705 m, sh, 690 m
$[Ph_2PCH_2CH_2PPh_2](CO)_2MnB_3H_8$	CH_2Cl_2 solution: 2530 mw, 2480 w, 2175 w, 1915 s, 1890 w, sh, 1490 w, 1440 m, 1190 vw, 1110 mw
	KBr mull: 3080 m, 3030 m, sh, 2965 mw, br, 2535 m, sh, 2480 s, 2395 m, 2165 m, 2025 mw, 1890 vs, 1575 mw, 1570 m, sh, 1485 m, 1435 m, 1420 m, 1390 m, sh, 1335 mw, 1310 w, 1275 w, 1190 m, 1160 mw, 1100 ms, 1080 m, 1050 w, 1030 mw, 1000 m, 990 s, sh, 965 m, sh, 915 mw, 875 mw, 850 mw, 815 m, 745 m, 690 s, 680 s, sh
$(CO)_3MnB_3H_8$	Gas phase, ~1.5 Torr: 2580 m, 2095 s, 1990 vs, 1965 mw, 1915 w, sh, 1880 mw, 790 w, 685 mw
	Thin film at −196 °C: 2560 s, 2475 w, sh, 2330 vw, 2165 mw, 2085 s, 1970 vs, 1895 ms, 1870 s, 1800 w, 1470 w, 1310 vw, 1260 mw, 1220 mw, 1185 m, sh, 1135 vw, 1045 mw, 1020 w, 955 m, 920 m, sh, 900 mw, 845 m, 785 ms, 685 ms
$(PF_3)(CO)_3MnB_3H_8$*	Gas phase, ~1.5 Torr: 2560 m, 2550 m, sh, 2500 m, 2205 mw, 2105 s, 2045 s, 1995 s, 1975 mw, 1830 mw, 1205 w, 1170 vw, 915 ms, 890 s, 865 m, sh, 840 w, sh, 745 w, 660 mw
	Thin film at −196 °C: 2545 s, 2480 s, 2195 ms, 2100 s, 2000 vs, 1825 ms, 1485 w, 1475 m, sh, 1430 w, 1320 vw, 1295 w, 1245 m, sh, 1205 m, 1160 m, 1055 mw, 1045 m, sh, 1010 m, 985 m, 960 m, 910 vs, 870 s, 835 ms, 815 w, sh, 765 vw, 700 ms
$(NH_3)(CO)_3MnB_3H_8$*	CH_2Cl_2 solution: 3460 w, sh, 3380 m, 3295 mw, 2545 m, 2490 ms, 2205 mw, 2075 s, 1955 vs, 1620 m, 970 vw, 850 vw
	KBr mull: 3450 m, sh, 3360 m, 3290 m, 3195 vw, 2515 s, sh, 2495 ms, 2460 ms, 2180 m, 2055 s, 1950 vs, 1615 m, 1315 vw, 1260 s, 1200 mw, 1170 mw, 1055 vw, 1035 vw, 1005 w, 960 w, 925 m, sh, 905 m, 845 mw
$(CO)_4MnB_3H_7Cl$	Thin film at −196 °C: 2545 mw, 2500 w, sh, 2215 vw, 2150 m, 2055 s, 2000 s, 1965 m, sh, 1830 vw, br, 1470 vw, 1060 mw, 960 vw, 920 w, 815 w, 755 vw, 700 s, sh
$(CO)_4MnB_3H_7Br$	KBr mull: 2530 s, 2455 w, sh, 2180 ms, 2130 s, 2050 vs, 1980 vs, 1825 m, 1445 m, br, 1200 mw, 1020 ms, 980 ms, 945 m, sh, 920 w, sh, 885 m, 810 m, 770 vw, 725 m
	CH_2Cl_2 solution: 2550 mw, 2200 vw, 2140 m, 2055 s, 2005 s, 1980 w, sh, 1825 vw, 1035 w

[a] The following abbreviations are used in the table: vs (very strong), s (strong), ms (medium strong), m (medium), mw (medium weak), w (weak), vw (very weak), sh (shoulder), br (broad). Unless otherwise noted frequencies are ±10 cm^{-1}. Gas-phase spectra were obtained at room temperature using 10-cm path length cells. The infrared data for the starred (*) complexes were obtained on samples composed of a mixture of isomers.

to significant product decomposition and formation of $HMn(CO)_5$ and $Mn_2(CO)_{10}$.

(2) Covalent B_3H_8 Complexes + $Mn(CO)_5X$. $(CH_3)_2AlB_3H_8$ and $(CH_3)_2GaB_3H_8$ are both volatile liquids and will react with $Mn(CO)_5X$ (X = Br, I) in the absence of solvent at elevated temperatures (~70 °C). In the absence of solvent, no significant reaction occurs between the two reagents at room temperature. This method of synthesis results in low yields and product mixtures that are hard to purify. Significant quantities of B_2H_6, $(CH_3)_3B$, and $HMn(CO)_5$ are formed.

The reaction between $(CH_3)_2AlB_3H_8$ or $(CH_3)_2GaB_3H_8$ and $Mn(CO)_5Br$ in methylene chloride or diethyl ether solution at room temperature produces up to a 94% yield of $(CO)_4MnB_3H_8$. Methylene chloride is the preferred solvent. The formation of B_2H_6, $HMn(CO)_5$, and $(CH_3)_2AlBr$ or $(CH_3)_2GaBr$ complicates the purification of the product.

The $(CO)_4MnB_3H_8$ is a yellow-orange liquid (mp +4 °C) having a vapor pressure of ~1 Torr at 20 °C. The neat liquid decomposes over a period of days upon exposure to air, becoming darker in color and more viscous. Methylene chloride solutions of $(CO)_4MnB_3H_8$, stored in screw-cap vials under an atmosphere of air, darken and deposit white solids over a period of several days. After 3 days infrared analyses showed $(CO)_4MnB_3H_8$ to be the major species present with a growing ν_{OH} absorption. Decomposition of the neat liquid in vacuo is very slow (5% in 4 days) at room temperature. The $(CO)_4MnB_3H_8$ is soluble in benzene, toluene, dichloromethane, diethyl ether, and tetrahydrofuran but decomposes upon refluxing in these solvents. Destruction of $(CO)_4MnB_3H_8$ occurs when it is heated at 100 °C as the neat liquid for 1 h in a closed system, with B_2H_6, $HMn(CO)_5$, and CO being the only identifiable volatile products. Reaction of $(CO)_4MnB_3H_8$ with $(CH_3)_3N$ or $(CH_3)_3P$ results in attack at the borane ligand with the formation of $(CH_3)_3N{\cdot}BH_3$ or $(CH_3)_3P{\cdot}BH_3$ as the major products. The mass spectrum of $(CO)_4MnB_3H_8$ exhibits a parent ion: $[(^{12}C^{16}O)_4{}^{55}Mn^{11}B_3{}^1H_8]^+$, found 208.0086 (calcd 208.0083).

$(CO)_4ReB_3H_8$. In a typical reaction $(CH_3)_4NB_3H_8$ (6.81 mmol), $Re(CO)_5Br$[25] (4.00 mmol), and about 15 mL of CH_2Cl_2 were stirred and UV irradiated in a quartz reaction flask for 27 h at room temperature. The $(CO)_4ReB_3H_8$ was purified on the vacuum line by distillation through a U-tube trap at 0 °C and condensation at −30 °C. A typical yield was 43%. $(CO)_4ReB_3H_8$ was also prepared in 7% yield directly from $Re_2(CO)_{10}$ and $(CH_3)_4NB_3H_8$ in CH_2Cl_2 solution using ultraviolet irradiation.

The $(CO)_4ReB_3H_8$ is a colorless liquid having a vapor pressure of approximately 0.5 Torr at 20 °C. The following parent fragment ions were identified in the mass spectrum of $(CO)_4ReB_3H_8$: $[(^{12}C^{16}O)_4{}^{187}Re^{11}B_3{}^1H_8]^+$, found 340.0256 (calcd 340.0262);

$[(^{12}C^{16}O)_4{}^{187}Re^{11}B_3{}^1H_6]^+$, found 338.0109 (calcd 338.0105); $[(^{12}C^{16}O)_4{}^{185}Re^{11}B_3{}^1H_6]^+$, found 336.0078 (calcd 336.0075). The product appears to be stable at room temperature in vacuo for several days with no significant decomposition. $(CO)_4ReB_3H_8$ is soluble in hydrocarbons, methylene chloride, and ethers. Attempted decarbonylation to produce $(CO)_3ReB_3H_8$ via passage of $(CO)_4ReB_3H_8$ through a glass bead packed hot tube at 200 °C on the vacuum line with continuous evacuation led to insignificant decomposition.

$(\eta^5\text{-}C_5H_5)(CO)FeB_3H_8$. In a typical preparation a 500-mL reaction vessel was charged with $(CH_3)_4NB_3H_8$ (52.1 mmol), $(\eta_5\text{-}C_5H_5)(CO)_2FeI$ (40.4 mmol), about 500 mL of CH_2Cl_2, a Teflon-coated magnetic stirring bar, and about twenty-five 4-mm borosilicate glass beads. The reaction mixture was UV irradiated under N_2 while stirring for 14 h at 15 °C, after which the ratio of $(\eta^5\text{-}C_5H_5)(CO)FeB_3H_8$ to unreacted $(\eta^5\text{-}C_5H_5)(CO)_2FeI$ was no longer changing (IR of the CO region). The methylene chloride solution was *rapidly* gravity filtered in air and the filtrate rotary evaporated to dryness. The crude product was sublimed at room temperature and 10^{-4} Torr to a probe cooled to −30 °C to give a 60% yield of $(\eta^5\text{-}C_5H_5)(CO)FeB_3H_8$ (which is only slightly more volatile than $(\eta^5\text{-}C_5H_5)(CO)_2FeI$).

$(\eta_5\text{-}C_5H_5)(CO)FeB_3H_8$ is a dark brown-black solid (mp 53–54 °C) that can be handled in air for short periods (~2 h). Deep purple-red solutions in hydrocarbons, methylene chloride, diethyl ether, and acetone are much more air sensitive. When the solid is allowed to stand at room temperature in vacuo over periods of days or weeks, a substantial fraction of the original complex is no longer sublimable. The decomposition product is a whitish gray solid.

Ultraviolet irradiation of CH_2Cl_2 solutions of $(\eta^5\text{-}C_5H_5)(CO)FeB_3H_8$ produced no conversion from bidentate to tridentate $B_3H_8^-$ functionality.

The mass spectrum of $(\eta^5\text{-}C_5H_5)(CO)FeB_3H_8$ exhibited a parent ion: $[(\eta^5\text{-}{}^{12}C_5{}^1H_5)(^{12}C^{16}O)^{56}Fe^{11}B_3{}^1H_8]^+$, found 190.0599 (calcd 190.0595).

$(H)(CO)_3FeB_3H_8$. In a typical reaction 15.23 mmol of $(CH_3)_4NB_3H_8$, 30 mL of CH_2Cl_2, and 6.07 mmol of $Fe(CO)_4Br_2$[26] were mixed at −78 °C in vacuo. From monitoring the amount of noncondensables produced, it was concluded that no reaction occurs below −50 °C and that the reaction is essentially complete after 1 h at −30 °C. The volatile contents of the reaction flask were transferred to the vacuum line with the reactor held below −20 °C in order to minimize decomposition of the product. Sizable quantities of B_2H_6 and B_4H_{10} were produced either during the reaction or during the transfer. The $(H)(CO)_3FeB_3H_8$ was purified by trap-to-trap distillation through a −30 °C U-trap and condensation in a −45 °C U-trap. Yields were greater than 30% but cannot be determined accurately due to the thermal instability of the complex.

At room temperature $(H)(CO)_3FeB_3H_8$ is a pale yellow liquid, soluble in CH_2Cl_2 and toluene. It is thermally unstable, decomposing slowly as the neat liquid even at −20 °C. Decomposition as the neat liquid or in solution is very rapid at room temperature. The major (>80%) borane-containing decomposition products are B_2H_6, B_4H_{10}, and $1\text{-}(CO)_3FeB_4H_8$.[5] Decomposition of $(H)(CO)_3FeB_3H_8$ is also accompanied by liberation of CO and H_2. $(H)(CO)_3FeB_3H_8$ is slightly more stable in the gas phase at room temperature and hence may be purified in the vacuum line.

The parent ion is not observed in the mass spectrum of $(H)(CO)_3FeB_3H_8$ at 18, 20, 30, or 70 eV, but the $[P - 1]^+$ ion is clearly visible. The ion of greatest intensity in the parent region of the mass spectrum corresponds to $[(^{12}C^{16}O)_3{}^{56}Fe^{11}B_3{}^1H_7]^+$: found 180.0023 (calcd 180.0023). Fragment envelopes corresponding to $[P - CO - H_2]^+$, $[P - 2CO - H_2]^+$, and $[P - 3CO - H_2]^+$ are visible in the mass spectrum.

$(\eta^5\text{-}C_5H_5)(CO)_2MoB_3H_8$. In a typical reaction a quartz reaction flask was charged with $(CH_3)_4NB_3H_8$ (7.60 mmol), $(\eta^5\text{-}C_5H_5)(CO)_3MoCl$ (4.91 mmol), and about 20 mL of CH_2Cl_2. The evolution of CO (~5.0 mmol) was complete in about 4.5 h. The methylene chloride solution was filtered under nitrogen into a Schlenk tube. The solvent was evaporated on the vacuum line and the residue remaining was transferred to a vacuum sublimator under nitrogen. Final purification by sublimation at room temperature (up to 40 °C) and 10^{-5} Torr to a −78 °C probe yielded small amounts (~5%) of the faintly pink solid product, $(\eta^5\text{-}C_5H_5)(CO)_2MoB_3H_8$, which is very air sensitive.

$(\eta^5\text{-}C_5H_5)(CO)_2WB_3H_8$. In a typical preparation a quartz reaction vessel was charged with $(CH_3)_4NB_3H_8$ (7.23 mmol), $(\eta^5\text{-}C_5H_5)(CO)_3WCl$ (5.04 mmol), and about 35 mL of CH_2Cl_2. After UV irradiation for 7 h at room temperature carbon monoxide evolution ceased. One mole of CO was produced per mole of $(\eta^5\text{-}C_5H_5)(CO)_3WCl$. As the reaction progressed, the solution color deepened from orange to dark red. After vacuum removal of solvent and $W(CO)_6$ the residue was extracted with CH_2Cl_2 and filtered and the filtrate adsorbed on predried Florisil. The complex was eluted from the chromatography column with tetrahydrofuran as a yellow band. Upon vacuum removal of the THF an orange-brown oil remained which possessed a ^{11}B NMR spectrum appropriate for $(\eta^5\text{-}C_5H_5)(CO)_2WB_3H_8$. Pure $(\eta^5\text{-}C_5H_5)(CO)_2WB_3H_8$ has not been isolated as a crystalline solid. Acetone solutions of $(\eta^5\text{-}C_5H_5)(CO)_2WB_3H_8$ appear to be air stable.

$(Ph_3P)(CO)_3MnB_3H_8$. In a typical reaction $(CH_3)_4NB_3H_8$ (9.62 mmol) and *trans*-$(Ph_3P)(CO)_4MnBr$[28] (6.57 mmol) reacted in vacuo in 30 mL of CH_2Cl_2 solvent. The reaction was complete in 22 h at room temperature in the dark. Gravity filtration of the reaction mixture, followed by solvent evaporation from the filtrate, gave 76% yield of an isomeric mixture of $(Ph_3P)(CO)_3MnB_3H_8$ as a yellow powder. Further purification was by column chromatography on Florisil using a 50/50 heptane/CH_2Cl_2 eluent. $(Ph_3P)(CO)_3MnB_3H_8$ is a bright light yellow solid which melts with decomposition at about 140 °C. The isomeric mixture is soluble in hydrocarbons and methylene chloride. The solid appears to be air stable for periods of hours, as are methylene chloride solutions.

$(Ph_2PCH_2CH_2PPh_2)(CO)_2MnB_3H_8$. Reaction between $(CH_3)_4NB_3H_8$ (6.40 mmol) and $(diphos)(CO)_3MnBr$ (4.07 mmol, diphos = $Ph_2PCH_2CH_2PPh_2$) in CH_2Cl_2 solution in vacuo was complete in 22 h at room temperature when the reaction was promoted by ultraviolet radiation. As the reaction proceeded, the solution color deepened from yellow-orange to red-orange. The residue in the reaction flask was taken up in CH_2Cl_2 and filtered, the solvent was evaporated from the filtrate, and the crude product was chromatographed on a Florisil column. The $(diphos)(CO)_2MnB_3H_8$ was collected, using CH_2Cl_2 eluent, in over 50% yield. The $(Ph_2PCH_2CH_2PPh_2)(CO)_2MnB_3H_8$ is an orange-pink solid that can be handled in air, both as the solid and in CH_2Cl_2 solution, for periods of hours without significant decomposition.

$(CO)_4MnB_3H_7Cl$. In a typical preparation 6.23 mmol of $(CO)_4MnB_3H_8$ and about 20 mL of CH_2Cl_2 were condensed in vacuo at −196 °C into a 200-mL reaction flask. The mixture was warmed and stirred to ensure solution homogeneity. Then 6.31 mmol of Cl_2 was condensed into the flask at −196 °C. The reaction flask was warmed from −78 °C to room temperature over a 5-h period and then held at room temperature for another 3.5 h. Less than 0.2 mmol of noncondensable gases was produced. The volatile contents in the reaction flask was transferred to the vacuum line. All of the chlorine was consumed, 6.30 mmol of HCl (~100%) was produced, and only a trace of $(CO)_4MnB_3H_8$ had not reacted. The yellow $(CO)_4MnB_3H_7Cl$ was isolated by condensation in a U-trap cooled to −15 °C. The small yield (10–20%) probably resulted from thermal decomposition of the neat product at room temperature. The $(CO)_4MnB_3H_7Cl$ appeared to be a yellow-orange solid at room temperature but was contaminated with a yellow liquid which was only very slightly more volatile than the orange solid. Evacuation of this mixture at room temperature enhanced the purity of the $(CO)_4MnB_3H_7Cl$, but the majority of it pumped away along with the impurity. This procedure did, however, provide pure samples of $(CO)_4MnB_3H_7Cl$ (as determined by NMR analysis).

$(CO)_4MnB_3H_7Cl$ exhibits no measurable vapor pressure at room temperature on an ordinary mercury manometer, but its air sensitivity necessitates its isolation using high-vacuum techniques. The exact *m/e* ratios were found for the following ions in the parent region of the 70-eV mass spectrum of $(CO)_4MnB_3H_7Cl$: $[(^{12}C^{16}O)_4{}^{55}Mn^{11}B_3{}^1H_7{}^{37}Cl]^+$, found 243.9685 (calcd 243.9664); $[(^{12}C^{16}O)_4{}^{55}Mn^{11}B_3{}^1H_7{}^{35}Cl]^+$, found 241.9693 (calcd 241.9693); $[(^{12}C^{16}O)_4{}^{55}Mn^{11}B_3{}^1H_5{}^{37}Cl]^+$, found 241.9495 (calcd 241.9507); $[(^{12}C^{16}O)_4{}^{55}Mn^{11}B_3{}^1H_5{}^{35}Cl]^+$, found 239.9524 (calcd 239.9536). The following ions or envelopes are present in the 70-eV mass spectrum: P^+ (P = parent ion), $[P - CO]^+$, $[P - 2CO]^+$, $[P - 3CO]^+$, $[P - 4CO]^+$, $[P - Cl]^+$, $[P - Cl - CO]^+$, $[P - Cl - 2CO]^+$, $[P - Cl - 3CO]^+$, $[P - Cl - 4CO]^+$, $(CO)MnB_2H_7^+$, MnH^+, Mn^+, HCl^+, and CO^+.

$(CO)_4MnB_3H_7Br$. In a typical preparation 10.15 mmol of Br_2 was condensed in vacuo on top of a frozen solution of 10.01 mmol of $(CO)_4MnB_3H_8$ in 20 mL of CH_2Cl_2 at −196 °C in a 200-mL reaction flask. The mixture was allowed to warm to room temperature, with stirring, over a 30-min period. During the last 10 min of this period the color of the reaction mixture lightened from its original reddish purple to dark orange. While the solution was at room temperature, the color continued to lighten for another 30 min until finally it was a light orange. Analysis of the volatile contents in the reaction flask revealed that all of the bromine had been consumed, 9.88 mmol of HBr (98.8%) had been formed, and only a trace of $(CO)_4MnB_3H_8$ had not reacted. After removal of the volatile products, $(CO)_4MnB_3H_7Br$ was isolated by extraction of the residue with CH_2Cl_2, filtration through a medium-porosity frit, and vacuum evaporation of the filtrate to dryness. The crude product was then purified by sublimation at 10^{-4} Torr at room temperature to a probe cooled at −78 °C. A higher purity product can be obtained via sublimation to a 0 °C probe. The yield of pure $(CO)_4MnB_3H_7Br$ was ~85%.

$(CO)_4MnB_3H_7Br$ is a light yellow solid (mp 48–49 °C dec) which is soluble in benzene, toluene, and methylene chloride. As the solid, $(CO)_4MnB_3H_7Br$ appears to be stable in dry air for days. Upon standing in air, CH_2Cl_2 solutions of $(CO)_4MnB_3H_7Br$ slowly deposit solid, but even after 4 h the majority of the $(CO)_4MnB_3H_7Br$ can be recovered unchanged. The mass spectrum of $(CO)_4MnB_3H_7Br$ exhibits a parent ion: $[(^{12}C^{16}O)_4{}^{55}Mn^{11}B_3{}^{1}H_7{}^{81}Br]^+$, found 287.9169 (calcd 287.9164). In an effort to convert the $B_3H_7Br^-$ ligand from bidentate to tridentate functionality, the decarbonylation of $(CO)_4MnB_3H_7Br$ was attempted. An all-quartz reaction tube, fitted with an O-ring Teflon valve, was charged with 4.62 mmol of $(CO)_4MnB_3H_7Br$ and 10 mL of CH_2Cl_2. The solution was irradiated with ultraviolet light for 22 h at room temperature. During this time approximately 5.7 mmol of carbon monoxide was evolved at a *steady* and *non*decreasing rate of 0.25 mmol/h, and an insoluble precipitate formed. The reaction was stopped at this point and the product mixture was analyzed. A mixture of $(CO)_4MnB_3H_8$ and $(CO)_3MnB_3H_8$ was produced in about 25% yield (1 mmol total). A small amount of B_2H_6 (0.5 mmol) was formed and a significant amount of $(CO)_4MnB_3H_7Br$ was recovered.

$(CO)_3MnB_3H_8$. Tricarbonyl[octahydrotriborato(1−)]manganese, $(CO)_3MnB_3H_8$, is prepared via photolytic or thermal decarbonylation of $(CO)_4MnB_3H_8$. The thermal procedure is preferred on the basis of simplicity, high yield, and ease of product purification.

Photolytic Decarbonylation of $(CO)_4MnB_3H_8$. (1) Solution Photolysis. In a typical preparation 5.56 mmol of $(CO)_4MnB_3H_8$ and 10 mL of CH_2Cl_2 were condensed into a 200-mL quartz reaction vessel. The mixture was stirred and irradiated in five 1-h stages in vacuo. The reaction mixture was cooled to −196 °C and the evolved carbon monoxide removed by evacuation after each hour of irradiation. As the irradiation progressed, the solution color darkened slightly from its original yellow-orange to a deeper yellow-orange and became cloudy. After 5 h of irradiation the contents of the flask were separated by distillation in the vacuum line. It is possible to obtain $(CO)_3MnB_3H_8$ in greater than 90% purity by multiple short-term distillations through a U-trap cooled at −36 °C or by use of a specially designed low-temperature distillation column.[27] The yield of $(CO)_3MnB_3H_8$ was 1.86 mmol, and 3.25 mmol of $(CO)_4MnB_3H_8$ was recovered. This corresponds to a 33% absolute yield of the product and an 81% yield based on $(CO)_4MnB_3H_8$ consumed in the reaction. A small quantity of $Mn_2(CO)_{10}$ is produced in the reaction.

(2) Gas-Phase Photolysis. The apparatus consists of a high-intensity ultraviolet source with U-tube traps adjacent on each side of the source; the whole apparatus is mounted on the vacuum line in such a way that the system can be evacuated from either end. The $(CO)_4MnB_3H_8$ is then condensed into one of the U-tube traps adjacent to the UV source. The trap on the other side of the source is cooled to −196 °C, the UV source is turned on, and then with continuous evacuation the $(CO)_4MnB_3H_8$ is distilled past the water-cooled UV source and condensed into the −196 °C trap. Once all of the $(CO)_4MnB_3H_8$ has been transferred, the direction of flow is reversed and passage in the opposite direction is carried out. Although efficient removal of carbon monoxide is achieved by this procedure, the rate of conversion from $(CO)_4MnB_3H_8$ to $(CO)_3MnB_3H_8$ is slow as a result of inefficient photon bombardment of $(CO)_4MnB_3H_8$, low gas-phase concentrations, and short residence times in the irradiation well. Thus many passages through the UV source (~2–4 days for a 10-mmol sample) are required to obtain $(CO)_3MnB_3H_8$ free of contamination with $(CO)_4MnB_3H_8$.

Thermal Decarbonylation of $(CO)_4MnB_3H_8$. Using the same basic procedure and setup described above for the gas-phase photolysis, except replacing the ultraviolet source with a hot tube packed with 4-mm glass beads at 180 °C, it is possible to obtain $(CO)_3MnB_3H_8$, in 80% yield, which is free of $(CO)_4MnB_3H_8$. Heating is accomplished by wrapping the pyrolysis tube in heating tape. The first pass through the hot tube requires several hours for ~10 mmol of starting material. The time needed for the subsequent passes decreases. Approximately five passes through the hot tube are required to ensure that all of the $(CO)_4MnB_3H_8$ has been converted to $(CO)_3MnB_3H_8$. The continuous vacuum removal of the evolved carbon monoxide is essential. The $(CO)_3MnB_3H_8$ is purified on the vacuum line by distillation through a U-tube trap cooled to −10 °C and condensation in a −45 °C U-tube trap. Small quantities of B_2H_6, $HMn(CO)_5$, and $Mn_2(CO)_{10}$ are also obtained. A shiny black residue coats the walls of the hot tube and the glass beads. Uniform melting of the material collected after passage through the hot tube indicates the completion of the decarbonylation.

When freshly purified, $(CO)_3MnB_3H_8$ is an air-sensitive, yellow-orange liquid (mp −7 °C). When the neat liquid stands in vacuo, its color darkens almost to red in a matter of hours at room temperature, but even after several days decomposition amounts to less than 10%. The vapor pressure of $(CO)_3MnB_3H_8$ is ~1.5 Torr at 20 °C, slightly greater than that of $(CO)_4MnB_3H_8$. It is soluble in hydrocarbons, methylene chloride, and ethers. THF solutions of $(CO)_3MnB_3H_8$ turn greenish brown after standing for 2 h at room temperature in vacuo, but the degree of decomposition is insignificant. Solutions in the other solvents are more resistant to color change. The mass spectrum of $(CO)_3MnB_3H_8$ exhibits a parent ion: $[(^{12}C^{16}O)_3{}^{55}Mn^{11}B_3{}^{1}H_8]^+$, found 180.0131 (calcd 180.0134).

$(CO)_3MnB_3H_8 + CO \rightarrow (CO)_4MnB_3H_8$. In a typical reaction 2.06 mmol of $(CO)_3MnB_3H_8$ and 10 mL of CH_2Cl_2 were condensed into a 300-mL Pyrex reaction flask. Carbon monoxide was then admitted to the reaction flask until its pressure reached 338 Torr, corresponding to 5.4 mmol. The flask valve was then closed and the solution allowed to stir at room temperature for 16 h. No $(CO)_3MnB_3H_8$ was recovered and 1.96 mmol of $(CO)_4MnB_3H_8$ (95%) was produced.

$(PF_3)(CO)_3MnB_3H_8$. In a typical reaction 2.01 mmol of $(CO)_3MnB_3H_8$, 2.59 mmol of PF_3, and 8 mL of CH_2Cl_2 were condensed into a 200-mL reaction flask and stirred at room temperature for 22 h. The solution color changed from its original yellow-orange to light yellow. There was 0.70 mmol of unreacted PF_3 recovered. No $(CO)_3MnB_3H_8$ was recovered but an isomeric mixture of $(PF_3)(CO)_3MnB_3H_8$, purified by distillation through a U-tube trap cooled to −16 °C and condensation in a U-tube trap at −50 °C, was isolated in 91% yield (1.83 mmol).

Alternatively, $(PF_3)(CO)_3MnB_3H_8$ can be prepared from $(CO)_3MnB_3H_8$ and excess PF_3 in the absence of solvent using the same reaction setup and conditions described above. The color of the reaction mixture darkens to a red-orange after 18 h at room temperature. All PF_3 in excess of the 1:1 stoichiometry is recovered. The yield of the isomeric mixture of $(PF_3)(CO)_3MnB_3H_8$ is comparable to that for the solution reaction.

$(PF_3)(CO)_3MnB_3H_8$ is a yellow-orange liquid at room temperature with a vapor pressure of ~1.5 Torr. It is soluble in hydrocarbons and methylene chloride. Decomposition as the neat liquid or in solution in vacuo amounts to only a few percent over a day at room temperature. The mass spectrum indicates that only the monosubstituted PF_3 derivative of $(CO)_3MnB_3H_8$ is formed, but NMR and IR spectroscopy show that a mixture of isomers is always produced. The mass spectrum exhibits a parent ion: $[(^{31}P^{19}F_3)(^{12}C^{16}O)_3{}^{55}Mn^{11}B_3{}^{1}H_8]^+$, found 267.9814 (calcd 267.9823).

$(NH_3)(CO)_3MnB_3H_8$. In a typical reaction a 100-mL reaction flask is charged with 4.39 mmol of $(CO)_3MnB_3H_8$, 4.36 mmol of NH_3, and approximately 20 mL of CH_2Cl_2. The stirred solution is warmed from −60 °C to room temperature over 8 h. The CH_2Cl_2 solution is filtered in air, the CH_2Cl_2 vacuum evaporated from the filtrate, and the crude solid dried under vacuum. A higher purity product is obtained by vacuum sublimation at 10^{-5} Torr and room temperature to a collection probe cooled to 0 °C (97% yield).

$(NH_3)(CO)_3MnB_3H_8$ is orange in crystalline form and appears to be air stable. It is soluble in benzene, toluene, and methylene chloride. The 70-eV mass spectrum of $(NH_3)(CO)_3MnB_3H_8$ displays a parent ion: $[(^{14}N^{1}H_3)(^{12}C^{16}O)_3{}^{55}Mn^{11}B_3{}^{1}H_8]^+$, found 197.0396 (calcd 197.0399). The spectrum contains fragments corresponding to the loss of NH_3 and the successive loss of each of the three carbon monoxide ligands.

Acknowledgment. This work was supported in part by grants, including departmental instrument grants for NMR and mass spectral facilities, from the National Science Foundation.

Registry No. $(CO)_4MnB_3H_8$, 53801-97-1; $(CO)_4ReB_3H_8$, 53801-98-2; $(\eta^5\text{-}C_5H_5)(CO)FeB_3H_8$, 53802-00-9; $(H)(CO)_3FeB_3H_8$, 65452-41-7; $(\eta^5\text{-}C_5H_5)(CO)_2MoB_3H_8$, 65452-40-6; $(\eta^5\text{-}C_5H_5)(CO)_2WB_3H_8$, 65452-39-3; $(Ph_3P)(CO)_3MnB_3H_8$, 65452-38-2; $(Ph_2PCH_2CH_2PPh_2)(CO)_2MnB_3H_8$, 65452-37-1; $(PF_3)(CO)_3MnB_3H_8$, 65452-36-0; $(NH_3)(CO)_3MnB_3H_8$, 65452-35-9; $(CO)_4MnB_3H_7Cl$, 65452-34-8; $(CO)_4MnB_3H_7Br$, 65452-33-7; $(CO)_4MnB_3H_7I$, 65452-32-6; $(CH_3)_4NB_3H_8$, 12386-10-6; $C_5B_3H_8$, 33220-36-9; TlB_3H_8, 12447-30-2; $(CH_3)_2AlB_3H_8$, 12654-95-4; $(CH_3)_2GaB_3H_8$, 12654-96-5; $Mn(CO)_5Br$, 14516-54-2; $Mn(CO)_5I$, 14879-42-6; $Re(CO)_5Br$, 14220-21-4; $(\eta^5\text{-}C_5H_5)(CO)_2FeI$, 12078-28-3; $Fe(CO)_4Br_2$, 14878-20-7; $(\eta^5\text{-}C_5H_5)(CO)_3MoCl$, 12128-23-3; $(\eta^5\text{-}C_5H_5)(CO)_3WCl$, 12128-24-4; *trans*-$(Ph_3P)(CO)_4MnBr$, 65437-12-9; (diphos)-$(CO)_3MnBr$, 19195-72-3; $(CO)_3MnB_3H_8$, 53801-96-0.

Supplementary Material Available: ^{1}H NMR, ^{11}B NMR, and mass spectra of some neutral octahydrotriborate(1−) complexes of chromium-, manganese-, and iron-group metals (9 pages). Ordering information is given on any current masthead page.

References and Notes

(1) (a) S. J. Lippard and D. Ucko, *Chem. Commun.*, 983 (1967); (b) *Inorg. Chem.*, 7, 1051 (1968); (c) S. J. Lippard and K. M. Melmed, *ibid.*, **8**, 2755 (1969).
(2) (a) F. Klanberg, E. L. Muetterties, and L. J. Guggenberger, *Inorg. Chem.*, 7, 2272 (1968); (b) F. Klanberg and L. J. Guggenberger, *Chem. Commun.*, 1293 (1967); (c) L. J. Guggenberger, *Inorg. Chem.*, **9**, 367 (1970).
(3) J. Borlin and D. F. Gaines, *J. Am. Chem. Soc.*, **94**, 1367 (1972).
(4) (a) D. F. Gaines and J. H. Morris, *J. Chem. Soc., Chem. Commun.*, 626 (1975); (b) J. C. Calabrese, D. F. Gaines, S. J. Hildebrandt, and J. H. Morris, *J. Am. Chem. Soc.*, **98**, 5489 (1976).
(5) N. N. Greenwood, C. G. Savory, R. N. Grimes, L. G. Snedden, A. Davison, and S. S. Wreford, *J. Chem. Soc., Chem. Commun.*, 718 (1974).
(6) S. J. Hildebrandt, D. F. Gaines, and J. C. Calabrese, *Inorg. Chem.*, companion paper in this issue.
(7) D. F. Gaines and S. J. Hildebrandt, *J. Am. Chem. Soc.*, **96**, 5574 (1974).
(8) A. O. Clouse, D. C. Moody, R. R. Rietz, T. Roseberry, and R. Schaeffer, *J. Am. Chem. Soc.*, **95**, 2496 (1973), and references therein.
(9) E. L. Muetterties, "Transition Metal Hydrides", Marcel Dekker, New York, N.Y., 1971, pp 76–78.
(10) G. R. Eaton, *J. Chem. Educ.*, **46**, 547 (1969).
(11) M. Suzuki and R. Kubo, *Mol. Phys.*, **7**, 201 (1963–1964).
(12) J. Bacon, R. J. Gillespie, and J. W. Quail, *Can. J. Chem.*, **41**, 3063 (1963).
(13) H. Beall and C. H. Bushweller, *Chem. Rev.*, **73**, 465 (1973).
(14) W. N. Lipscomb and G. R. Eaton, "NMR Studies of Boron Hydrides and Related Compounds", W. A. Benjamin, New York, N.Y., 1969.
(15) W. N. Lipscomb, *Adv. Inorg. Chem. Radiochem.*, **1**, 117 (1959). See also I. M. Pepperberg, T. A. Halgren, and W. N. Lipscomb, *Inorg. Chem.*, **16**, 363 (1977).
(16) Preliminary x-ray analysis of $(CO)_4MnB_3H_7Br$ indicates that the halogen atom is in the exo position as shown in Figure 1c.
(17) Chemical shifts are positive downfield from $BF_3{\cdot}O(C_2H_5)_2 = 0.0$, the opposite of previous usage: *J. Organomet. Chem.*, **131**, C43 (1977).
(18) (a) D. Marynick and T. Onak, *J. Chem. Soc. A*, 1160 (1970); (b) H. Beall, C. Bushweller, W. Dewkett, and M. Grace, *J. Am. Chem. Soc.*, **92**, 3484 (1970); (c) C. H. Bushweller, H. Beall, M. Grace, W. Dewkett, and H. Bilofsky, *ibid.*, **93**, 2145 (1971).
(19) W. J. Dewkett, M. Grace, and H. Beall, *Inorg. Synth.*, **15**, 115 (1974).
(20) A saturated aqueous solution of $(CH_3)_4NCl$ was added to the diglyme solution of NaB_3H_8. The product was recrystallized from hot methanol.
(21) E. Amberger and E. Gut, *Chem. Ber.*, **101**, 1200 (1968).
(22) Additional NMR and mass spectra are included in the supplementary material.
(23) D. F. Shriver, "The Manipulation of Air-Sensitive Compounds", McGraw-Hill, New York, N.Y., 1969.
(24) E. W. Abel and G. Wilkinson, *J. Chem. Soc.*, 1501 (1959).
(25) Prepared from $Re_2(CO)_{10}$ and Br_2 via the same procedure employed for $Mn(CO)_5Br$ (see ref 22).
(26) G. Brauer, "Handbook of Preparative Inorganic Chemistry", 2nd ed, Academic Press, New York, N.Y., 1963, p 1350.
(27) D. F. Gaines, design to be submitted for publication.

Contribution from the Department of Chemistry,
University of Wisconsin, Madison, Wisconsin 53706

Kinetics of the Isomerization of 1-Chloro- and 2-Chloropentaborane(9) Using Diethyl Ether Catalyst

D. F. GAINES* and J. L. WALSH

Received July 8, 1977

The isomerization of 1-chloro- or 2-chloropentaborane(9), $1\text{-}ClB_5H_8$ or $2\text{-}ClB_5H_8$, with diethyl ether catalyst is approximately first order in ClB_5H_8 and in diethyl ether. For the reaction

$$1\text{-}ClB_5H_8 + Et_2O \underset{k'_{21}}{\overset{k'_{12}}{\rightleftharpoons}} 2\text{-}ClB_5H_8 + Et_2O$$

at 24.5 °C, 0.174 M $1\text{-}ClB_5H_8$, and 3.65 M Et_2O, the overall second-order rate constants are $k'_{12} = 2.72\ (3) \times 10^{-6}\ M^{-1}\ s^{-1}$, $k'_{21} = 0.48\ (1) \times 10^{-6}\ M^{-1}\ s^{-1}$, and $K_{eq}\ (=k'_{12}/k'_{21}) = 5.62$. The activation energy for the forward reaction is 14.6 (5) kcal. The data suggest that the isomerization occurs by a boron cage rearrangement mechanism involving an $Et_2O{-}ClB_5H_8$ complex rather than a mechanism involving B–Cl bond cleavage.

Introduction

The mechanism by which 1- and 2-substituted pentaboranes isomerize has not been well characterized experimentally. One mechanism which has been proposed for the isomerizations involves polyhedral rearrangement.[1] The square-pyramidal substituted pentaborane(9) has been proposed[1] to rearrange through a trigonal-bipyramidal intermediate which allows interconversion of apical and basal boron atoms and, thus, isomerization of 1- or 2-substituted species.

This stereochemical nonrigidity in polyhedral structures is an interesting and important aspect of inorganic chemistry. Mechanistic models[2] for interconversion of structures with diamond and square faces have been proposed to describe possible pathways for low-energy rearrangement of polyhedral species. Other polytopal rearrangement processes have been described[3] for polyhedral cage molecules and coordination complexes. The most favorable geometric arrangement of a five-vertex polyhedron[3,4] is, theoretically, a trigonal bipyramid but a tetragonal pyramid is only slightly less favorable. The atom movement required to interchange structures with these geometries is small, little more than bending or stretching motions in the molecules. Interchange of trigonal-bipyramidal and tetragonal-pyramidal geometries can be rapid with resulting interchange of all sites in the molecules. Such a mechanism, proposed by Berry,[5] is illustrated in Figure 1. The proposed rearrangement which occurs during isomerization of pentaborane(9) species[1] is closely related to that illustrated in Figure 1. However, the tetragonal pyramid is found to be

0020-1669/78/1317-0806$01.00/0